Resilient Design Coalition

BUCKLING RESTRAINED BRACED FRAME FUNCTIONAL RECOVERY PREQUALIFICATION

Final Report Submitted to the PUC (1/5/2026) for Consideration in the 2026 NEHRP Provisions

CHARLES PANKOW FOUNDATION
Building Innovation through Research

Seismic Performance Prediction Platform
by Haselton Baker Risk Group

kpff

UBC

FUNCTIONAL RECOVERY PREQUALIFICATION REPORT FOR BUCKLING RESTRAINED BRACED FRAMES

Final Report Submitted to the PUC for Consideration in the 2026 NEHRP Provisions

Prepared By:

Resilient Design Coalition

Financially Supported by:

CoreBrace and the Charles Pankow Foundation

TECHNICAL WORK AND AUTHORSHIP BY:

Ed Almeter, MS
Kristen Blowes, PhD, PE
Jared DeBock, PhD, PE
Curt Haselton, PhD, PE
Carlos Molina Hutt, PhD, PE
Huy Pham, PhD
David Welch, PhD
Reid Zimmerman, SE

January 5, 2026

RDC

QUANTIFICATION OF FUNCTIONAL RECOVERY SEISMIC PERFORMANCE FACTORS FOR BUCKLING RESTRAINED BRACED FRAME BUILDINGS

Submitted: 1/5/2026

EXECUTIVE SUMMARY

A quantification of the functional recovery seismic performance factors for the Buckling-Restrained Braced Frame (BRBF) lateral forced resisting system is performed in accordance with the proposed Section A.8.3.6 procedures in Appendix A of the 2026 National Earthquake Hazards Reduction Program (NEHRP) Provisions. The assessments documented herein covers the design of buildings with BRBF lateral force resisting systems designed according to Chapter 12 of ASCE 7-22, considering configurations with fixed beam-to-column connections and those with pinned connections in the lateral bays. Design coefficients and factors for life-safety design are based on line B.26 of Table 12.2-1 in ASCE 7-22, "Steel buckling restrained braced frames." The response modification factor, R, is 8, overstrength factor, Ω, is 2.5, and the deflection amplification factor, C_d, is 5.0. All designs investigated herein satisfy the life-safety design provisions of ASCE 7-22.

Appendix A of the 2026 NEHRP Provisions provides additional design requirements to satisfy functional recovery performance objectives at the Functional Recovery Earthquake (FRE_R) level shaking. The functional recovery seismic performance factors include the functional recovery response modification coefficient, R_{fr}, functional recovery allowable story drift limit, Δ_{afr}, and the functional recovery structure ductility reduction factor, $R_{\mu fr}$. Drift checks are performed with C_d equal to R_{fr} for functional recovery design.

$R_{fr,}$ and Δ_{afr} were determined by developing an archetype space of different building heights, designed with various functional recovery response modification coefficients and allowable drift limits, and then selecting the combination that results in less than a 10% mean probability of Safety-Critical Structural Damage, or P[SCSD], in each performance group, and less than 20% P[SCSD] for any individual archetype, for Functional Recovery Category (FRC) A, B and C. The 10% and 20% thresholds are modified to 15% and 25%, respectively, for FRC D. All analyses are conducted at the Functional Recovery Earthquake (FRE_R) level shaking corresponding to a Seismic Design Category $D_{max,FRE}$ condition with two-point spectral ordinates S_{dsfr} and S_{d1fr} of 1.25g and 0.75g, respectively. The required values of $R_{fr,}$ and Δ_{afr} based on analysis are compared to the judgment-based limits according to Appendix A of NEHRP 2026, and the more stringent values are selected. The judgment-based limits of R_{fr} are R/1.5 and R/1.25 for FRC A/B/C and FRC D, respectively. The judgment-based limits of Δ_{afr} are 1.25% and 1.75% for FRC A/B/C and FRC D, respectively. System specific $R_{\mu fr}$ factors are determined by comparing peak floor acceleration demands from the analysis with the seismic floor

accelerations from Section A.10.6 in accordance with Section A.8.3.6 procedures in Appendix A of the 2026 NEHRP Provisions.

Results from the assessment showed that the functional recovery performance factors for BRBFs were primarily governed by the need to limit residual drifts in the buildings. This study finds that residual drifts in BRBF's are most influenced by: (1) The drift limit; stiffening the building by reducing Δ_{afr} reduces residual drifts in BRBF buildings. (2) Strength; increasing the strength of BRBF buildings by reducing R_{fr} decreases yielding and drift concentrations in the lower stories, lowering the likelihood of residual drift. (3) Fixed vs. pinned connections of BRBF beams and columns; BRBFs with surrounding framing that uses fixed beam-to-column connections benefit from stronger restoring forces provided by the frame and exhibit greater resistance to residual drift.

The proposed R_{fr}, Δ_{afr}, and $R_{\mu fr}$ for the Buckling-Restrained Braced Frame (BRBF) lateral force resisting system from the qualification assessment are presented in Table 1 and Table 2 for configurations with and without fixed beam-to-column connections, respectively. For BRBF's with fixed beam-to-column connections, a drift limit of Δ_{afr} equal to 1% achieves the performance goals for FRC A/B/C and FRC D, without needing to reduce R_{fr} below the judgment-based limits of R/1.5 = 5.5 and R/1.25 = 6.5 respectively. For BRBF's with pinned beam-to-column connections, drift limit of Δ_{afr} equal to 0.75% is required to further limit residual drifts, with R_{fr} equal to 5.5 and 6.0 for FRC A/B/C and FRC D, respectively.

Table 1 - Summary of functional recovery seismic performance factors for BRBF lateral systems with fixed beam-to-column connections (BRBF-M).

	FRC A/B/C			FRC D		
	R_{fr}	**Δ_{afr}**	**$R_{\mu fr}$**	**R_{fr}**	**Δ_{afr}**	**$R_{\mu fr}$**
Analysis results	6.5	1.00%	--[†]	7	1.00%	--[†]
Judgment-based upper limit	5.5	1.25%	n/a	6.5	1.75%	n/a
Recommendation – BRBF with fixed beam-to-column connections	**5.5**	**1.00%**	**1.25**	**6.5**	**1.00%**	**1.25**

[†]$R_{\mu fr}$ is only calculated for the recommended seismic performance factors

Table 2 - Summary of functional recovery seismic performance factors for BRBF lateral systems with pinned beam-to-column connections (BRBF-S).

	FRC A/B/C			FRC D		
	R_{fr}	**Δ_{afr}**	**$R_{\mu fr}$**	**R_{fr}**	**Δ_{afr}**	**$R_{\mu fr}$**
Analysis results	5.5	0.75%	--[†]	6.0	0.75%	--[†]
Judgment-based upper limit	5.5	1.25%	n/a	6.5	1.75%	n/a
Recommendation – BRBF with pinned beam-to-column connections	**5.5**	**0.75%**	**1.15**	**6.0**	**0.75%**	**1.20**

[†]$R_{\mu fr}$ is only calculated for the recommended seismic performance factors

Contents

1. INTRODUCTION

This report documents the quantification of the functional recovery seismic performance factors for the BRBF system. Quantification of the functional recovery seismic performance factors is performed in accordance with the proposed Section A.8.3.6 procedures of the 2026 National Earthquake Hazards Reduction Program (NEHRP) Provisions. The functional recovery seismic performance factors include the functional recovery response modification coefficient, R_{fr}, the functional recovery allowable story drift limit, Δ_{afr}, and the functional recovery structure ductility reduction factor, $R_{\mu fr}$. These are the equivalents of the response modification coefficient, R, the allowable story drift limit, Δ_a, and the structure ductility reduction factor, R_μ, used in ASCE/SEI 7 Chapters 12 and 13, but for design for functional recovery.

An archetype space of different building heights, designed with various functional recovery response modification coefficients and allowable drift limits was developed. FEMA P-58/ATC-138 (FEMA, 2018; ATC, 2021) models were then created. In accordance with the proposed Section A.8.3.6 procedures of the 2026 NEHRP Provisions, only structural components are included in these FEMA P-58/ATC-138 performance models. Design of the archetypes was performed using the automated design capability of SP3 (www.sp3risk.com) and engineering demand parameters (e.g., story drift ratios, wall chord rotations, coupling beam rotations, etc.) were estimated using SP3's Response Prediction Engine, which while calibrated based on extensive nonlinear response history analyses, does not perform nonlinear response history analyses of the specific archetype directly. Analyses are conducted following FEMA P-58 and ATC-138 recommendations except as documented otherwise in this report. Using the FEMA P-58/ATC-138 performance models, the probability of safety-critical structural damage (P[SCSD]) was then calculated for each archetype. P[SCSD] is shown to directly correlate with the probability of exceeding a functional recovery time of up to 2 months when using structural-only models in the ATC-138 framework (Blowes et al., in review).

The functional recovery seismic performance factors are selected such that archetypes designed for that R_{fr} and Δ_{afr} result in less than a 10% mean P[SCSD] in each performance group and less than 20% P[SCSD] for any individual archetype for Functional Recovery Category (FRC) A, B and C. The 10% and 20% thresholds are modified to 15% and 25%, respectively, for FRC D. These limits are in accordance with the proposed Section A.8.3.6 procedures of the 2026 National Earthquake Hazards Reduction Program (NEHRP) Provisions. All analyses are conducted at the Functional Recovery Earthquake (FRE_R) level shaking corresponding to a Seismic Design Category $D_{max,FRE}$ condition with two-point spectral ordinates S_{dsfr} and S_{d1fr} of 1.25g and 0.75g, respectively.

2. ANALYSIS METHODS

2.1. Design Iteration and Acceptance Criteria for Seismic Performance Factors

For each individual archetype, design iterations are carried out using values of R_{fr} and Δ_{afr} across the ranges of 1 through R (i.e., up to the response modification coefficient used in life-safety design) and 0.5% through 2.0% (i.e., up to the maximum allowable story drift ratio for Risk Category II structures), respectively. The Response Modification Factor, R, is 8 for BRBF systems, in accordance with Table 12.2-1 of ASCE 7-22 (ASCE, 2022). These design iterations are performed using the SP3 design engine that estimates strength and stiffness of each design to estimate appropriate structural responses and subsequent estimates of SCSD.

In each performance group, the combination of R_{fr} and Δ_{afr} is deemed to be acceptable if the mean P[SCSD] is less than 10%, and the maximum P[SCSD] across all archetypes in the performance group is less than 20% for quantifying the functional recovery seismic performance factors for Functional Recovery Category (FRC) A, B and C. For FRC D, the mean and maximum P[SCSD] across all archetypes in a performance group must be less than 15% and 25%, respectively. The recommended design values for a particular system are taken as the most restrictive across all performance groups, rounded to the nearest increment considered (0.25 for R_{fr} and 0.25% for Δ_{afr}).

The requirements of the proposed Section A.8.3.6 procedures of the 2026 NEHRP Provisions impose that R_{fr} and Δ_{afr} shall not be taken less than R/1.5 and 1.25% for FRC A, B and C and R/1.25 and 1.75% for FRC D. These "judgment-based" upper limits on seismic performance factors correspond to values required for Risk Category IV (FRC A, B, and C) and Risk Category III (FRC D) structures when performing life safety design. Additionally, to verify the strength and stiffness coupling inherent to each design variant, each archetype model is re-assessed under an independent strength and stiffness assumption, i.e., where additional strength prescribed by R_{fr} does not add additional stiffness to the building. Analysis outcomes from the independent-strength-and-stiffness assessment are checked to ensure the maximum P[SCSD] does not exceed the acceptance criteria (20% for FRC A/B/C and 25% for FRC D), where applicable. The judgment-based upper limit and the independent-strength-and-stiffness check provide a reasonable limit, preventing too great of a reliance on the analytical results and recognizing the historical precedent set by the higher Risk Categories.

2.1.1. Safety-Critical Structural Damage (SCSD)

The triggering of SCSD is governed by the assigned safety class for a given component and damage state according to the ATC-138 methodology (ATC, 2021). The safety class controls the percent of components, in each story and direction, that can be in each damage state or greater, prior to triggering SCSD. A summary of the ATC-138 safety class descriptions and acceptance thresholds is shown in Table 3.

Table 3. ATC-138 safety-class definitions for triggering SCSD (ATC, 2021).

Safety Class	Description	Acceptance Threshold[a]
0	Slight damage that is not a safety concern and will never trigger an unsafe placard	N/A
1	Moderate damage that may be visually concerning, but does not substantially reduce the lateral strength of the component.	50%
2	Severe damage that causes substantial loss of lateral strength of the component, but does not substantially reduce its vertical load carrying capacity.	25%
3	Severe damage that compromises both lateral and vertical load carrying capacity of the component.	10%

[a] Percentages reflect the upper quantity of components, in each story and direction, that can be in a safety class of interest before triggering safety-critical structural damage (SCSD). The safety critical structural damage check is performed independently for each independent system in the building (e.g., the gravity vs. lateral system).

2.2. Fragility Functions for BRBFs

Fragility functions are used to relate structural responses to likely damage and consequences. Fragility functions are commonly modeled by a lognormal distribution defined by a lognormal mean (θ) and standard deviation (β). For a given structural component, sequential damage states (DSs) can be represented by individual fragility functions that represent the likelihood of a distinct level of damage and corresponding level of repair effort and consequences. Additionally, damage states may be mutually exclusive, where a single fragility function may be used to represent multiple outcomes (i.e., sub-damage states) where the likelihood of each is given a weighting that sums to unity (e.g., 0.25 + 0.75 = 1). The fragility functions used in the current study will use both sequential and mutually exclusive damage state definitions. More general background information on fragility functions and damage state development can be found in FEMA P-58-1 (FEMA, 2018).

The following sub-sections provide details on the structural component fragility functions, including:

- Buckling restrained brace assemblies with simple beam connections;
- Buckling restrained brace assemblies with moment connections;
- Bolted shear tab gravity connections;
- Column base plates;

- Welded column splices.

Foundation elements are considered rugged in the current analysis. Fragility functions for foundation elements were not developed during the FEMA P-58 project and foundations elements are specifically included in the list of acceptable rugged components in Appendix I of FEMA P-58-1 (FEMA, 2018a). Further, the estimation of structural responses assumes a fixed base condition at grade, without any consideration of foundation flexibility or soil structure interaction. Gravity framing (e.g., beams and columns) is assumed rugged other than beam-to-column gravity connections.

2.2.1. Buckling Restrained Brace Fragilities

Fragility functions for buckling-restrained braces (BRBs) used in this study were developed in two stages including direct work by Haselton Baker Risk Group for CoreBrace (Wade, 2017; Almeter et al. 2018) and as part of the ATC-138 Project (ATC, 2021; Welch and Deierlein, 2024).

BRBs are assumed to comply with the stability and testing requirements of AISC 341-22 (AISC, 2022). Fragility functions for BRBs are developed for simply-connected and moment-connected beam-to-column connections within the braced bay. The damage state hierarchy consists of two sequential damage states (i.e., DS1 and DS2). DS1 is split into three mutually exclusive damage states (i.e., DS1a, DS1b, DS1c). DS2 represents the failure of the BRB itself, while DS1 represents possible damage scenarios in the surrounding frame and connections depending on the type of beam-to-column connections. BRBs with moment connections tend to have lower DS1 drift capacity than simply-connected BRBs as moment-connected beams force larger strains into the beam flanges and gusset welds. BRBs with simply-connected beams tend to have higher inherent flexibility.

Examples of damage to the BRBF components associated with DS1 are provided in Figure 1. In ATC 138, DS1c and DS2 are assigned a Safety Class of 2, indicating a questionable residual lateral strength of the frame. Summaries of the fragility functions are provided in Table 4 and Table 5 for simply-connected and moment-connected beams, respectively. The median story drift ratio for DS2 is a function of brace configuration, brace connection type, story height, bay length, and steel core area.

Table 4. BRB with simply-connected beams fragility damage states and corresponding safety classes.

Damage State[a]	Median (θ)[b]	β	Safety Class[c]	Damage Description	Repair Measures
DS1a (0.5)	3.5%	0.3	0	Initial yielding of the gusset is possible. Yielding has initiated in framing at gusset plates but no buckling has occurred. No repairs required.	Damage in field is either obscured or deemed to not warrant repair. No repair conducted.
DS1b (0.25)	3.5%	0.3	0	Cracking and tearing of welds and gussets adjacent to welds but crack length is less than critical for fracture. Significant yielding and local buckling in beams and columns adjacent to gusset.	Repair gusset welds and heat straighten gussets, if necessary. Frame members require heat straightening but additional stiffening likely not required. BRB is salvageable.
DS1c (0.25)	3.5%	0.3	2	Severe yielding and buckling of beams and columns adjacent to the gusset with possibility of local tearing in buckled areas. Onset of weld fracture and buckling possible in gusset plates. Remaining lateral strength of BRB system is questionable.	Gusset and gusset welds are severely damaged, likely requiring replacement. Yielding and local buckling of beams and columns may be repaired by heat straightening, stiffeners, or reinforcement, if there is no cracking or tearing. If cracking or tearing has initiated more substantial repair is needed. BRB is salvageable.
DS2	Varies [d]	0.3 1	2	Fracture of brace or gusset. Buckling of gusset. Severe yielding of beams and columns adjacent to the gusset with possibility of local buckling and cracking in the yielded areas. Severe loss of lateral resistance.	Brace and gusset are severely damaged with significant loss in stiffness and resistance, and both likely require replacement. Yielding and local buckling of beams and columns may be repaired by heat straightening, stiffeners, or reinforcement, if there is no cracking or tearing. If cracking or tearing has initiated more substantial repair is needed.

[a] Mutually exclusive damage states (e.g., DSXa and DSXb) include the probability of occurrence in parentheses
[b] Fragility function is a lognormal distribution with median and standard deviation of θ and β, respectively. The EDP is story drift ratio.
[c] SC 1 = 50%, SC 2 = 25%, SC 3 = 10% allowable quantity of damaged components per direction per story; SC 0 does not cause SCSD.
[d] Median for DS2 depends on bay geometry, BRB-to-gusset connection, and steel core area (see Table 6).

Table 5. BRB with moment-connected beams fragility damage states and corresponding safety classes.

Damage State[a]	Median (θ)[b]	β	Safety Class[c]	Damage Description	Repair Measures
DS1a (0.5)	3.0%	0.3	0	Cracking and tearing of welds and gussets adjacent to welds but crack length is less than critical for fracture. Significant yielding and local buckling in beams and columns adjacent to gusset.	Repair gusset welds and heat straighten gussets, if necessary. Frame members require heat straightening but additional stiffening likely not required. BRB is salvageable.
DS1b (0.25)	3.0%	0.3	0	Severe yielding and buckling of beams and columns adjacent to the gusset with possibility of local tearing in buckled areas. Onset of weld fracture and buckling possible in gusset plates.	Gusset and gusset welds are severely damaged, likely requiring replacement. Yielding and local buckling of beams and columns may be repaired by heat straightening, stiffeners or reinforcement, if there is no cracking or tearing. If cracking or tearing has initiated more substantial repair is needed. BRB is salvageable.
DS1c (0.25)	3.0%	0.3	2	Severe yielding and buckling of beams and columns adjacent to the gusset with possibility of local tearing in buckled areas. Onset of weld fracture and buckling possible in gusset plates. Remaining lateral strength of BRB system is questionable.	Gusset and gusset welds are severely damaged, likely requiring replacement. Yielding and local buckling of beams and columns may be repaired by heat straightening, stiffeners or reinforcement, if there is no cracking or tearing. If cracking or tearing has initiated more substantial repair is needed. BRB is salvageable.
DS2	Varies [d]	0.31	2	Fracture of brace or gusset. Buckling of gusset. Severe yielding of beams and columns adjacent to the gusset with possibility of local buckling and cracking in the yielded areas. Severe loss of lateral resistance.	Brace and gusset are severely damaged with significant loss in stiffness and resistance, and both likely require replacement. Yielding and local buckling of beams and columns may be repaired by heat straightening, stiffeners or reinforcement, if there is no cracking or tearing. If cracking or tearing has initiated more substantial repair is needed.

[a] Mutually exclusive damage states (e.g., DSXa and DSXb) include the probability of occurrence in parentheses
[b] Fragility function is a lognormal distribution with median and standard deviation of θ and β, respectively. The EDP is story drift ratio.
[c] SC 1 = 50%, SC 2 = 25%, SC 3 = 10% allowable quantity of damaged components per direction per story; SC 0 does not cause SCSD.
[d] Median for DS2 depends on bay geometry, BRB-to-gusset connection, and steel core area (see Table 6).

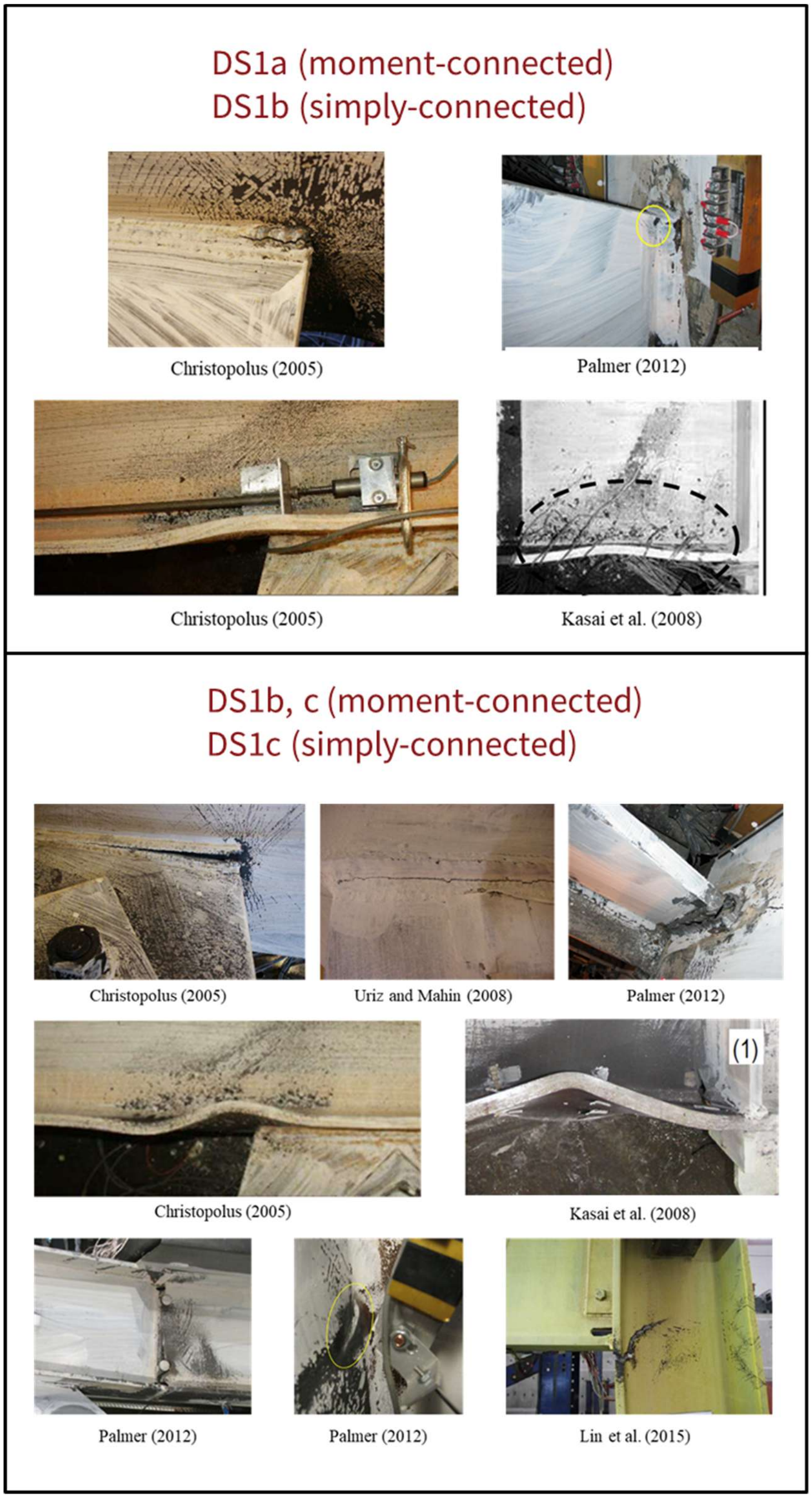

Figure 1 – Illustrations of buckling-restrained brace frame DS1 sub-damage states listed in Tables 3 and 4 (Welch and Deierlein, 2024).

The development of the DS2 fragilities was performed by Wade (Wade, 2017; Almeter et al. 2018) working directly with CoreBrace. The DS2 fragilities are based on a median strain capacity of 3.5% that was estimated from a collection of 17 CoreBrace BRB assembly (i.e., brace and connections) tests. Tests included a variety of connection types (e.g., welded, bolted, pinned) and a range of steel core areas (A_{sc}) of 1 in^2 to 27 in^2 (14 in^2 on average). The strain demand was converted to an equivalent story drift ratio based on the assumed bay geometry, BRB-to-gusset connection, steel core area, and brace configuration. A total of 132 different fragilities were developed to cover the range used in design. A key parameter for the story drift ratio conversion is the yield length ratio (YLR) that represents the ratio of the steel core length (L_{sc}) to the work point length of the brace (L_{wp}). The YLR is governed by numerous factors, with the steel core area (A_{sc}) and BRB-to-gusset connection type having the greatest influence. An increase in A_{sc} requires more of the available length (L_{wp}) to be used by the connections and stiffeners outside of the principal core area. An illustration of the relationships used to convert BRB strain (ε) to story drift ratio (SDR) is provided in Figure 2.

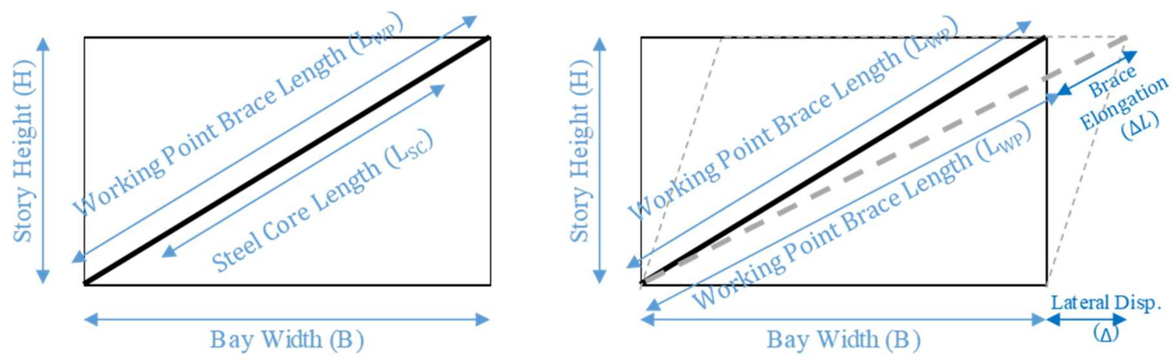

$$\Delta L = \varepsilon L_{SC} \qquad \Delta = \sqrt{\left(L_{wp} + \Delta L\right)^2 - H^2} - B \qquad SDR = \frac{\Delta}{H}$$

Figure 2 – Conversion of BRB strain to story drift ratio (adapted from Wade, 2017). Note that the illustration is for a diagonal configuration spanning the entire bay length.

The full set of available DS2 fragilities consider numerous BRBF configuration options:

- Brace configuration (Diagonal or Chevron);
- Story height (14 ft, 16 ft, 20 ft);
- Bay width (20 ft or 30 ft for Diagonal; 30 ft or 40 ft for Chevron);
- BRB-to-gusset connection (Bolted, Pinned, Welded);
- Steel core area (5 in^2, 10 in^2, 20 in^2, 30 in^2).

The current study considers both diagonal and chevron configurations with story heights of 14 or 16 feet (see Section 2.3 for full archetype discussion). Diagonal configurations assume a 20-foot bay length while chevron configurations assume a 30-foot bay length, which is assumed representative. BRB-to-gusset connections are limited to bolted connections on the basis that this connection type is the most conservative in terms for drift capacity and are, by far, the most common connection type used in design (Saxey, 2024). The median story drift ratios corresponding to DS2 for the range of configurations used in this study are provided in Table 6, noting that the type of beam-to-column connection does not affect the DS2 capacity. Fragility comparisons of upper and lower DS2 capacities for the range considered are presented for simply-connected and moment-connected BRBF assemblies in Figure 3 and Figure 4, respectively.

Table 6. Median DS2 drift capacities for the range of BRBs considered for archetype buildings

Configuration	**Brace Connection**	**h_{st} [ft]**	**L_{bay} [ft]**	**A_{sc} [in^2]**	**θ_{DS2} [%]**
Diagonal	Bolted	16	20	5	5.4%
				10	4.9%
				20	4.8%
				30	4.4%
Diagonal	Bolted	14	20	5	5.4%
				10	4.9%
				20	4.7%
				30	4.4%
Chevron	Bolted	16	30	5	5.2%
				10	4.7%
				20	4.5%
				30	4.2%
Chevron	Bolted	14	30	5	5.1%
				10	4.6%
				20	4.4%
				30	4.1%

[a] h_{st} = story height, L_{bay} = bay length, A_{sc} = steel core area, θ_{DS2} = median drift capacity for damage state 2

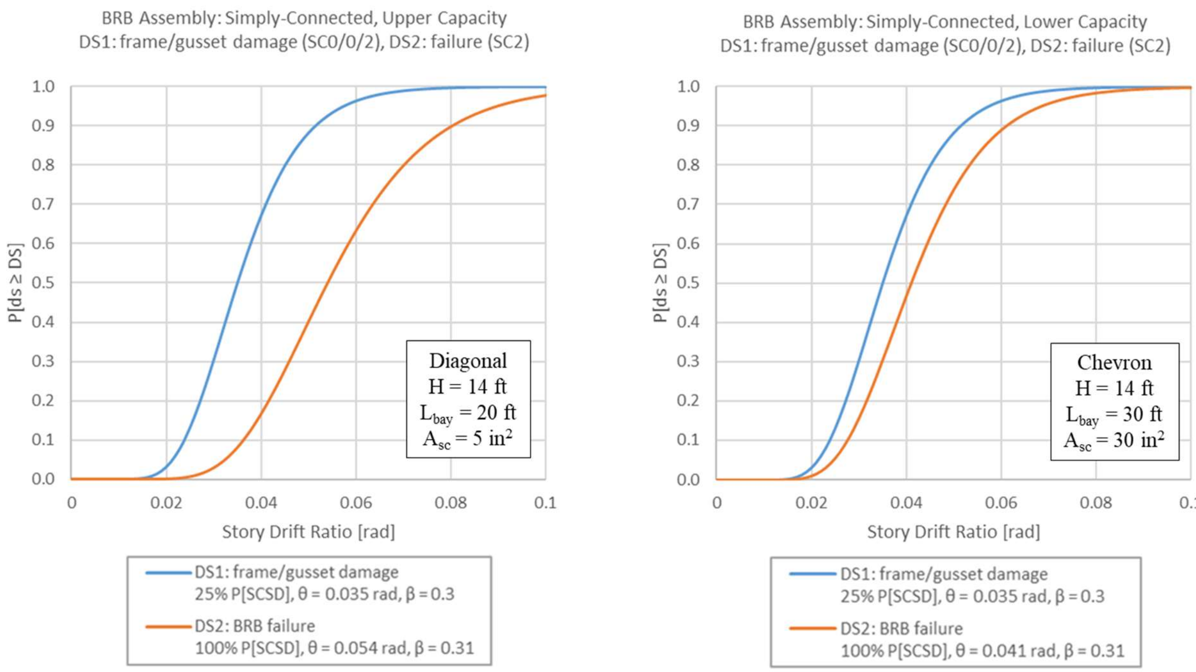

Figure 3 – Fragility functions for simply-connected BRBF assemblies: upper DS2 capacity (left), lower DS2 capacity (right)

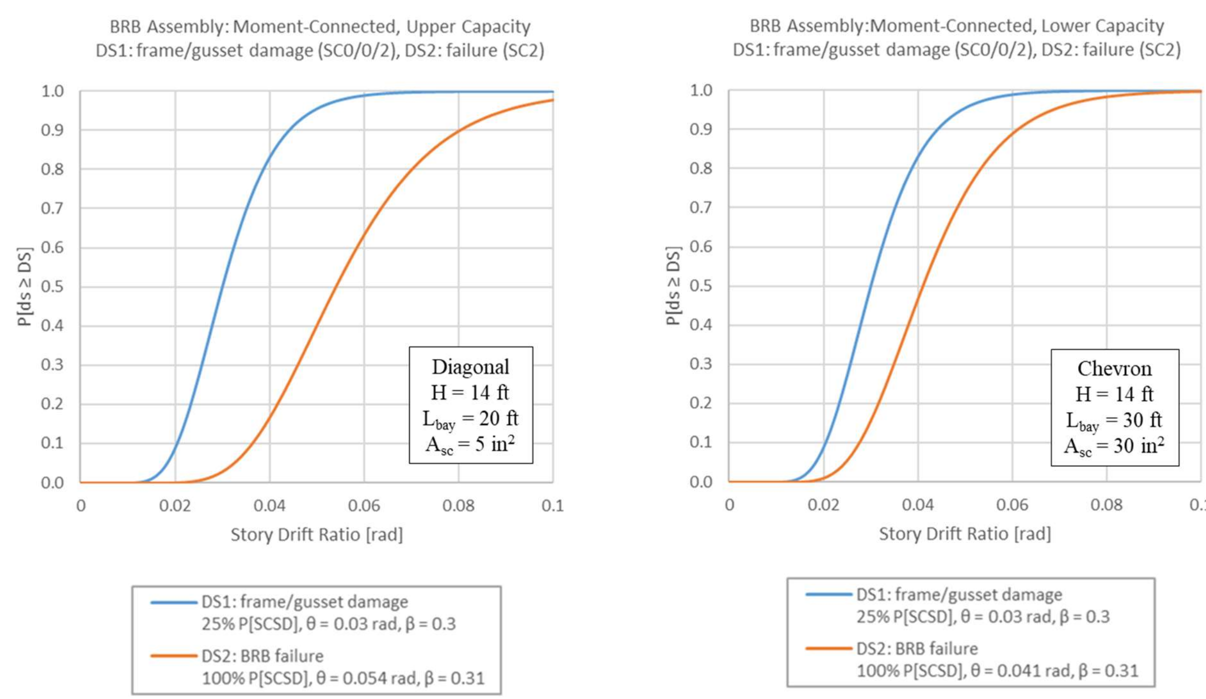

Figure 4 – Fragility functions for moment-connected BRBF assemblies: upper DS2 capacity (left), lower DS2 capacity (right)

The development of DS1 fragilities for BRBFs was conducted during the ATC-138 project (ATC, 2021; Welch and Deierlein, 2024) motivated by two key observations:

- FEMA P-58 fragilities for BRBFs (added in 2018) were based on judgment without an experimental basis. The original fragilities had a single damage state representing the complete failure of the BRB with a median story drift ratio of 2%, which was based on typical drift limits and did not reflect the testing requirements, specifically, AISC 341-22 (AISC, 2022) requires BRBs to be successfully tested to a minimum drift demand of 2%.
- Experimental testing of BRBF assemblies (i.e., full frame tests) revealed the possibility of different types of damage prior to full failure of the BRB itself, including out-of-plane failure of gusset and stiffener sections, frame damage, and damage to gusset plates.

The DS1 fragilities are based on an extensive review of experimental testing on full BRBF assemblies as well as review of current code requirements for BRBF design. Table 7 and Table 8 summarize the experimental tests results forming the basis for onset of damage (DS1a for moment-connected frames and DS1b for simply-connected frames) and significant damage (DS1b and DS1c for moment-connected frames and DS1c for simply-connected frames.), respectively (Tables 3 and 4 from Welch and Deierlein, 2024).

Table 7 – Experimental summary corresponding to DS1a for moment-connected frames and DS1b for simply-connected frames.

Reference	Specimen	Damage Description	BRB connection	Beam to Column Connection	Config.	Story Drift Ratio [rad]
Christopolus (2005)	C-Ref	Weld damage, visible frame buckling (~t_{flange})	Bolted	Welded	Diagonal	0.0182
	C-2	Visible frame buckling (~t_{flange}), significant yielding	Bolted	Welded	Diagonal	0.0193
	C-3	Weld damage, visible frame buckling (~t_{flange})	Bolted	Welded	Diagonal	0.0173
	C-4	Weld damage, visible frame buckling (~t_{flange})	Bolted	Welded	Diagonal	0.0192
	C-1	Visible frame buckling (~t_{flange}), Significant yielding	Bolted	Welded	Diagonal	0.0206
Palmer (2012)	Frame 1	Weld damage	Pinned	Welded	Diagonal	0.0190
	Frame B	Weld damage	Pinned	Welded	Diagonal	0.0180
Uriz and Mahin (2008)	UM-1	Fracture of column stiffener	Welded	Welded	Diagonal	0.0202
	UM-2	Initial weld damage	Welded	Welded	Diagonal	0.0173
	UM-3	Beam weld damage	Welded	Welded	Diagonal	0.0173
Kasai et al. (2008)	3	Visible frame buckling (~t_{flange})	Bolted	Welded	Diagonal	0.0200
Chou et al. (2012)	5	Gusset weld damage	Bolted	Welded	Diagonal	0.0200

Lin et al. (2012)	Hybrid2	Initial weld damage	Welded	Welded	Chevron	0.0200
Lin et al. (2015)	Stage 1	Initial weld damage	Welded	Welded	Chevron	0.0193

Table 8 - Experimental summary corresponding to DS1b & DS1c for moment-connected frames and DS1c for simply-connected frames.

Reference	Specimen	Damage Description	BRB connection	Beam to Column Connection	Config.	Story Drift Ratio [rad]
Christopolus (2005)	C-Ref	Beam buckling and OOP distortion; column flange buckling; significant weld damage	Bolted	Welded	Diagonal	0.0194
	C-2	Beam and column flange buckling (both ends); significant weld damage	Bolted	Welded	Diagonal	0.0220
	C-3	Weld damage both ends, severe buckling in column flange	Bolted	Welded	Diagonal	0.0199
	C-4	Severe buckling in beam flange; weld failure	Bolted	Welded	Diagonal	0.0224
	C-1	Severe buckling in beam flange; buckling in beam web; onset of beam flange fracture	Bolted	Welded	Diagonal	0.0290
Palmer (2012)	Frame 1	Gusset weld fracture; column flange buckling; beam flange buckling	Pinned	Welded	Diagonal	0.0270
	Frame B	Beam flange tearing; gusset weld fracture; column flange tearing	Pinned	Welded	Diagonal	0.0300
Uriz and Mahin (2008)	UM-2	Gusset buckling; weld damage	Welded	Welded	Diagonal	0.0259
	UM-3	Weld damage; fracture of beam flange	Welded	Welded	Diagonal	0.0216
Kasai et al. (2008)	3	Significant beam flange damage	Bolted	Welded	Diagonal	0.0300
Berman and Bruneau (2009)	BB-1	Failure of unconstrained beam-to-column connection; column base fracture	Bolted	Unconstrained welded	Diagonal	0.0290
Chou et al. (2012)	1	Crack in beam web near cope	Bolted	Welded	Diagonal	0.0200
	5	Crack in beam flange; gusset weld tears	Bolted	Welded	Diagonal	0.0250
Lin et al. (2012)	Cyclic	Lower gusset fracture in first story	Welded	Welded	Chevron	0.0320
	Cyclic	Upper gusset fracture in second story	Welded	Welded	Chevron	0.0310
Lin et al. (2015)	Stage 1	Column flange fracture	Welded	Welded	Chevron	0.0200

	Stage 2	Significant beam buckling; column flange/web fracture	Welded	Welded	Chevron	0.0290

The current DS1 fragilities used in this study assume that all the stability requirements of ASIC 341-22 are satisfied, which directly target eliminating early failure modes, such as out-of-plane buckling, that do not allow the full capacity of the BRB core to be reached; observations of damage related to instability issues from experimental tests (Table 5 from Welch and Deierlein, 2024) were excluded in the development of the DS1 fragilities used in this study. Non-conforming BRBF designs may be more susceptible to these types of failures. More details on the development of DS1 fragilities can be found in Welch and Deierlein (2024).

2.2.2. Steel Gravity Connection Fragilities

Steel gravity beam-to-column connections are based on fragility development by Deierlein and Victorsson (2008) during the FEMA P-58 Project and are available within the FEMA P-58 fragility database. The fragilities are based on thirteen experimental tests on simple bolted shear tab connections conducted by Liu and Astaneh (2000). Fragilities are developed using story drift ratio as the EDP.

Fragility functions for steel gravity connections are comprised of three sequential damage states with DS1 split into two mutually exclusive DSs to either conduct or neglect minor repairs. DS2 is assigned a Safety Class of 2, while DS3 is assigned a Safety Class of 3. ATC-138 assigned Safety Class 2 to both DS2 and DS3. Following review of the damage description for DS3, the Safety Class was increased to 3 to be more in line with the Safety Class definitions (see Table 3) based on the judgment of the review committee. A summary of the fragility functions and corresponding safety class assignments is provided in Table 9. Figure 5 shows example photographs of each damage state. A plot of the fragility functions is provided in Figure 6.

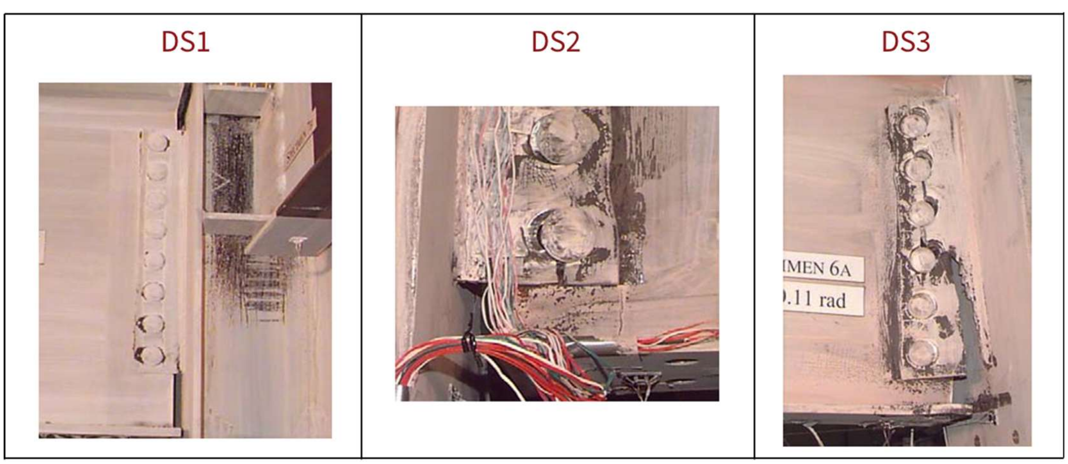

Figure 5 – Illustration of damage states for steel shear tab connections (Deierlein and Victorsson, 2008).

Table 9. Bolted shear tab gravity connection fragility damage states and corresponding safety classes.

Damage State[a]	Median (θ)[b]	β	Safety Class[c]	Damage Description	Repair Measures
DS1a (0.95)	4.00%	0.4	0	Yielding of shear tab and elongation of bolt holes, possible crack initiation around bolt holes or at shear tab weld. Damage in field is either obscured or deemed to not warrant repair. No repair conducted.	Careful inspection and welded repair to any cracks and possible replacement of shear tab if bolt hole deformations are excessive (possible for deeper 6-bolt or deeper shear tabs). Field condition is deemed to not warrant repair by field observation.
DS1b (0.05)	4.00%	0.4	0	Yielding of shear tab and elongation of bolt holes, possible crack initiation around bolt holes or at shear tab weld.	Careful inspection and welded repair to any cracks and possible replacement of shear tab if bolt hole deformations are excessive (possible for 6-bolt or deeper shear tabs).
DS2	8.00%	0.4	2	Partial tearing of shear tab and possibility of bolt shear failure (6-bolt or deeper connections).	Repairs will include either welded repair of shear tab or possible complete replacement of shear tab and installation of new bolts. Repairs may require shoring of beam.
DS3	11.00%	0.4	3[d]	Complete separation of shear tab, close to complete loss of vertical load resistance.	Repair will include complete replacement of shear tab and installation of new bolts. Repairs will require shoring of beam.

[a] Mutually exclusive damage states (e.g., DSXa and DSXb) include the probability of occurrence in parentheses
[b] Fragility function is a lognormal distribution with median and standard deviation of θ and β, respectively. The EDP is story drift ratio.
[c] SC 1 = 50%, SC 2 = 25%, SC 3 = 10% allowable quantity of damaged components per direction per story; SC 0 does not result in SCSD.
[d] This assessment deviates from the ATC 138 assignment of DS3 as Safety Class 2 based a review of the safety class definitions and the judgment of the authors.

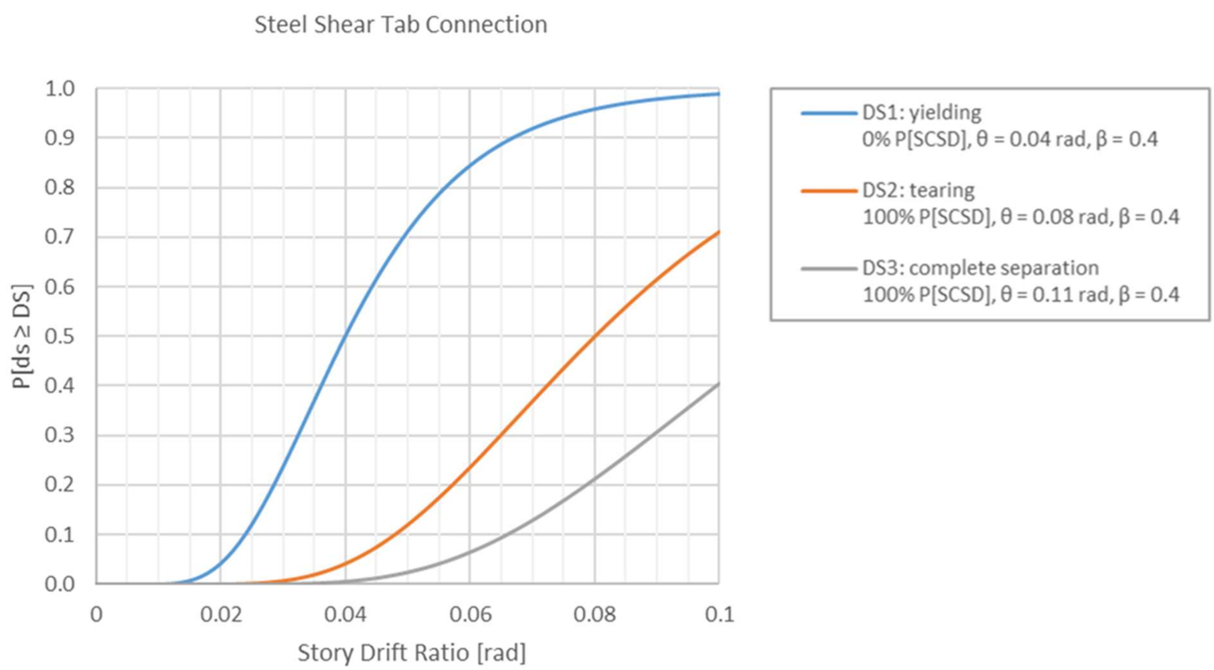

Figure 6 – Fragility functions for bolted shear tab gravity connections.

2.2.3. Steel Column Baseplate Fragilities

Steel column baseplates are based on fragility development by Deierlein and Victorsson (2008) during the FEMA P-58 Project and are available within the FEMA P-58 fragility database. The fragilities are based on thirteen experimental tests on exposed column baseplates reported by three studies (Burda and Itani, 1999; Fahmy, 1999; Hajjar et al. 2005). All tests considered loading in the strong axis direction of the column. Fragilities are developed using story drift ratio as the EDP.

Fragility functions for steel column baseplate connections are comprised of three sequential damage states with DS1 split into two mutually exclusive DSs to either conduct or neglect minor repairs. DS2 is associated with crack propagation into the column or baseplate. DS3 represents the complete fracture and dislocation of the column. DS2 and DS3 are assigned Safety Classes of 2 and 3, respectively. A summary of the fragility functions is provided in Table 10.

Table 10. Steel column baseplate connection fragility damage states and corresponding safety classes.

Damage State[a]	Median (θ)[b]	β	Safety Class[c]	Damage Description	Repair Measures
DS1a (0.95)	4.00%	0.4	0	Initiation of crack at the fusion line between the column flange and the base plate weld. Damage in field is either obscured or deemed to not warrant repair. No repair conducted.	The repair will involve removal of a portion of grade slab, gouging out material surrounding the fracture initiating and re-welding, then repair of slab. Field condition is deemed to not warrant repair by field observation.
DS1b (0.05)	4.00%	0.4	0	Initiation of crack at the fusion line between the column flange and the base plate weld.	The repair will involve removal of a portion of grade slab, gouging out material surrounding the fracture initiating and re-welding, then repair of slab.
DS2	7.00%	0.4	2	Propagation of brittle crack into column and/or base plate.	Depending on the crack trajectory, the repair will range from replacement of a portion of the column or base plate to full replacement of the column base. Replacement will require shoring of column, torch cutting to remove damaged material, and fabrication and field welding to install replacement material.
DS3	10.00%	0.4	3	Complete fracture of the column (or column weld) and dislocation of column relative to the base.	Repair would likely involve replacing the entire base plate assembly and most of the column in the story above the base plate.

[a] Mutually exclusive damage states (e.g., DSXa and DSXb) include the probability of occurrence in parentheses

[b] Fragility function is a lognormal distribution with median and standard deviation of θ and β, respectively. The EDP is story drift ratio.

[c] SC 1 = 50%, SC 2 = 25%, SC 3 = 10% allowable quantity of damaged components per direction per story; SC 0 does not result in SCSD.

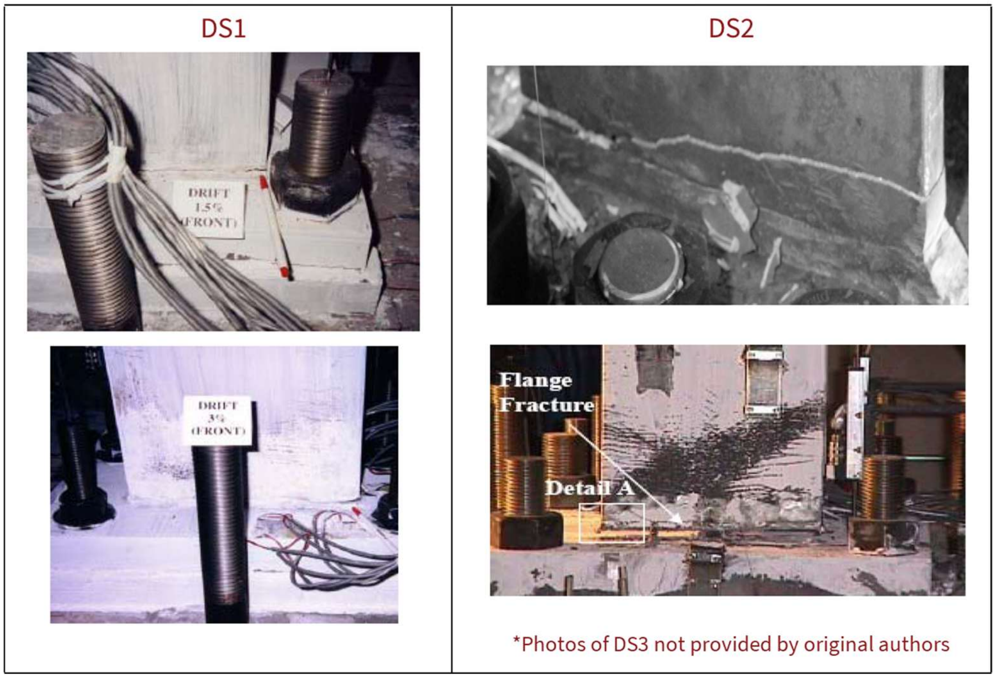

Figure 7 – Illustration of the first two damage states for steel column baseplates (Deierlein and Victorsson, 2008).

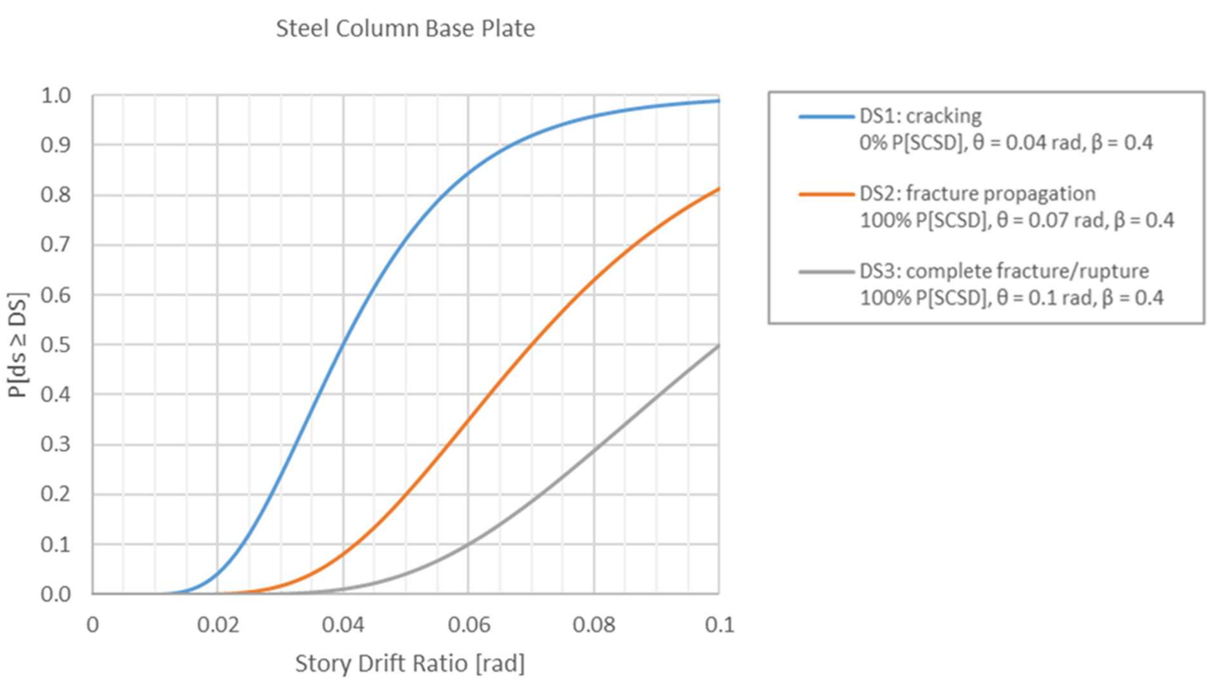

Figure 8 – Fragility functions for steel column baseplates.

2.2.4. Welded Column Splice Fragilities

Steel welded column splices are based on fragility development by Deierlein and Victorsson (2008) during the FEMA P-58 Project and are available within the FEMA P-58 fragility database. The fragilities are based on experimental testing conducted by Bruneau et al. (1987) and fracture analysis performed by Nuttayasakul (2001). Fragilities are developed using story drift ratio as the EDP.

Fragility functions for welded steel column splices are comprised of two sequential damage states with DS1 split into two mutually exclusive DSs to either conduct or neglect minor repairs. DS2 represents complete fracture of the splice and is attributed a Safety Class of 3. A summary of the fragility functions is provided in Table 11. A plot of the fragility functions is provided in Figure 9. Notably, original documentation for these fragilities did not provide photographs of damage states.

Table 11. Welded column splice fragility damage states and corresponding safety classes.

Damage State[a]	**Median (θ)**[b]	**β**	**Safety Class**[c]	**Damage Description**	**Repair Measures**
DS1a (0.95)	2.00%	0.4	0	Ductile fracture of the groove weld flange splice. Damage in field is either obscured or deemed to not warrant repair. No repair conducted.	Repair would involve gouging out the material adjacent to the fracture and repairing with a new groove weld. Field condition is deemed to not warrant repair by field observation.
DS1b (0.05)	2.00%	0.4	0	Ductile fracture of the groove weld flange splice.	Repair would involve gouging out the material adjacent to the fracture and repairing with a new groove weld.
DS2	5.00%	0.4	3	DS1 followed by complete failure of the web splice plate and dislocation of the two column segments on either side of the splice.	Repair may not be practically feasible, but would require either realignment or replacement of adjacent column segments and rewelding of splice.

[a] Mutually exclusive damage states (e.g., DSXa and DSXb) include the probability of occurrence in parentheses

[b] Fragility function is a lognormal distribution with median and standard deviation of θ and β, respectively. The EDP is story drift ratio.

[c] SC 1 = 50%, SC 2 = 25%, SC 3 = 10% allowable quantity of damaged components per direction per story; SC 0 does not result in SCSD.

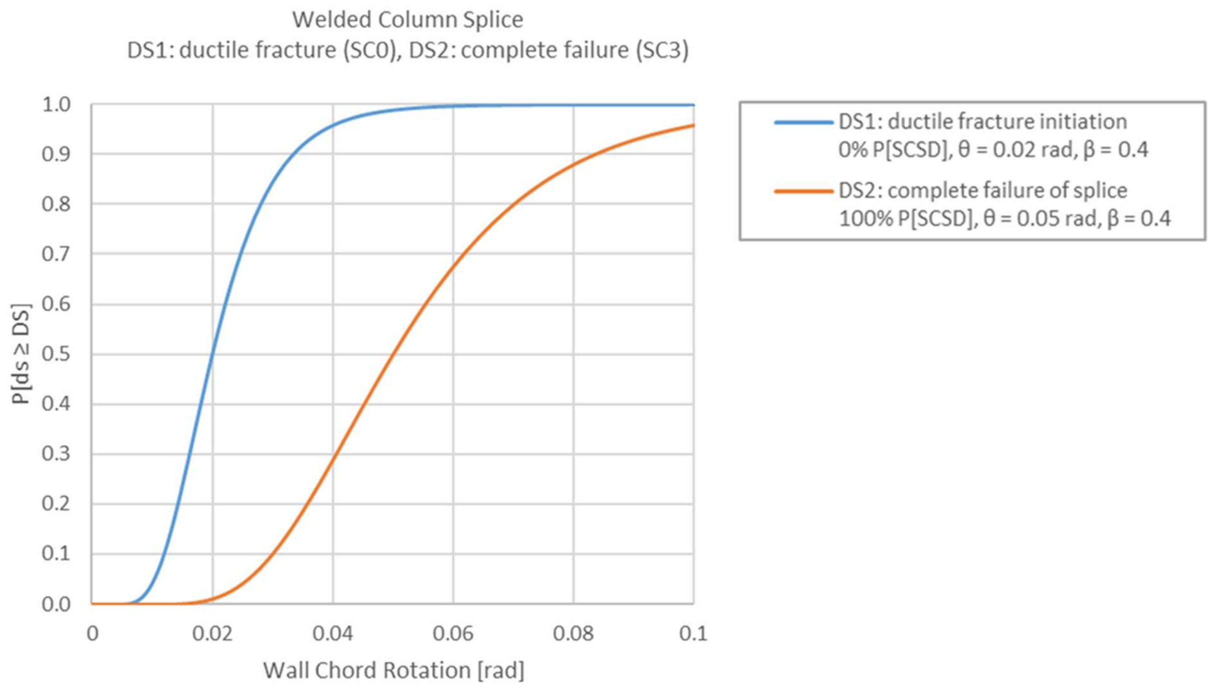

Figure 9 – Fragility functions for welded column splices.

2.3. Archetypes Considered for Analysis

To determine the combination of R_{fr} and Δ_{afr} that results in acceptable functional recovery performance, an archetype space is broken up into performance groups, analyzed, and the overall parameters are determined by the worst-case of the performance groups. This is similar to the FEMA P695 methodology used for quantifying performance factors for life-safety (FEMA, 2009) and is in accordance with the proposed Section A.8.3.6 procedures of the 2026 NEHRP Provisions.

The BRBF system has an archetype space comprised of six different performance groups and a total of 72 individual archetype variants. The background on the development of the archetype design space is presented in the following sub-sections.

2.3.1. Building Configuration and Structural Component Population

All archetypes assume a constant plan area of 100 feet by 100 feet. Story heights are assumed to be 16 and 14 feet for the first and typical stories, respectively. This selection of story heights is consistent with the definition of the BRBF fragility assemblies discussed in Section 2.2.1.

The following archetype variables are considered:

- Number of stories;
- BRB configuration;
- Number of braced bays per direction;
- Beam-to-column connection within the BRBF.

Building heights range from 2 to 16 stories, split into three height classes: low-rise (2, 3, and 4 stories), mid-rise (6, 8 and 10 stories), and high-rise (12 and 16 stories). BRB configurations are diagonal and chevron. The braced bay length is 20 feet and 30 feet for diagonal and chevron configurations, respectively. Each brace configuration considers two or four braced bays per direction of the building. The variation of number of braced bays allows for a range of steel core areas (e.g., brace sizes) that can affect the fragility of the BRBF assembly (see Section 2.2.1). Reducing the number of braced bays simulates investigating a larger plan size, from a fragility selection standpoint, even if two braced bays per side and direction is more common. Each BRBF variation considers either simple beam-to-column connections (i.e., no backup frame) or moment connections (i.e., with backup frame) within the braced bays.

Typical plan layouts and populated structural components are shown in Figure 10. Steel shear tab gravity connections are assumed at every location outside of the BRBFs. Column base plates are populated at each base column within a BRBF bay. Elevation views of diagonal and chevron BRBFs are shown for a 6-story archetype in Figure 11. Welded column splices are populated at every second story for columns within each BRBF bay (see Figure 11).

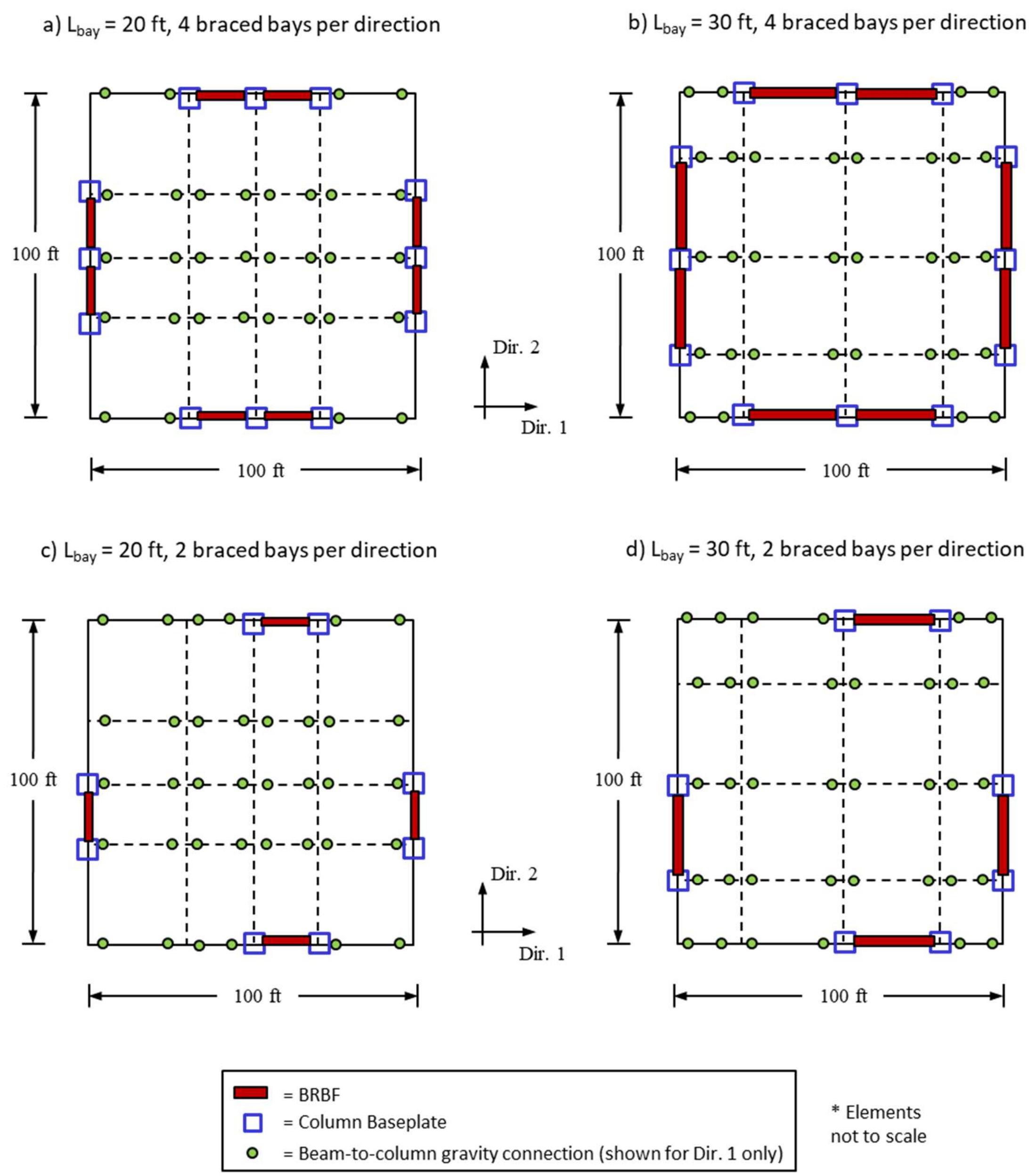

Figure 10 – Illustration of assumed plan layouts for BRBF archetypes with population of structural components.

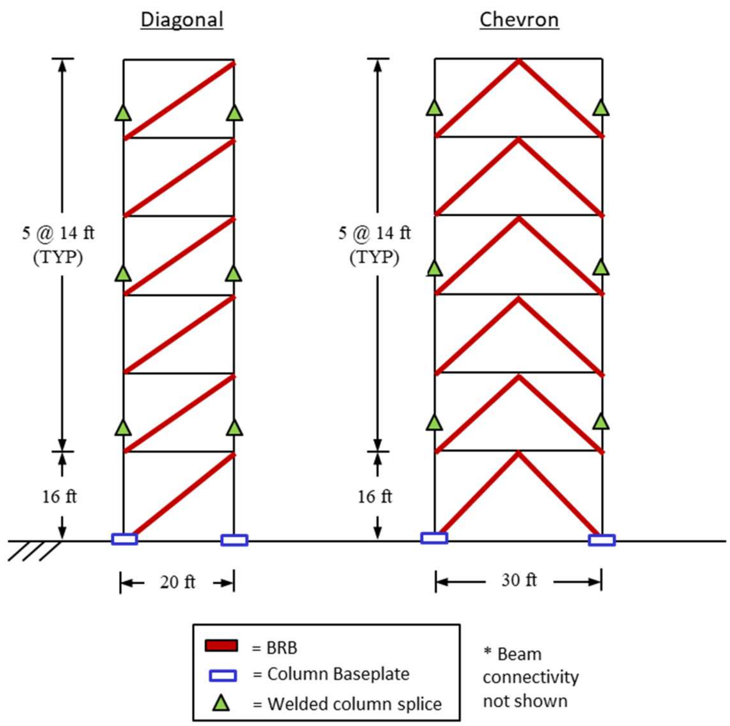

Figure 11 – Elevation views of 6-story BRBFs with populated structural components: diagonal (left) and chevron (right) configurations.

2.3.2. Performance Groups for BRBF

Performance groups are delineated based on building characteristics that influence the structural properties and global response of BRBF buildings; these include building height and beam-to-column connectivity (pinned vs. moment connected).

The performance group heights considered were low-rise (PG1), mid-rise (PG2) and high-rise (PG3). The use of building height to define (or delineate) performance groups has a strong precedence in numerous applications of the FEMA P-695 methodology, which serves as a basis of the performance group concept used in the current study and underlying NEHRP Appendix A provisions. As a minimum, performance groups are distinguished between short-period (short structures) and long-period (tall structures).

Performance groups are further discretized according to the type of beam-to-column connection within the BRBF, because the beam-to-column connection influences residual drift response. Pinned beam-to-column connections provide less restoring force and therefore have higher expected residual drift.

The number of braced bays and the brace configuration were varied within each performance group. These characteristics affect the component fragilities, but do not significantly impact global structural properties or building response.

The definition of each performance group is shown in Table 12.

Table 12. BRBF performance group summary.

Performance Group	Description	No. Stories	Brace Configurations [a]	No. Braced Bays [b]	No. per PG
PG1-BRB-M	Low-rise – Moment-connected	2, 3, 4	Diagonal, Chevron	2, 4	12
PG2-BRB-M	Mid-rise – Moment-connected	6, 8, 10	Diagonal, Chevron	2, 4	12
PG3-BRB-M	High-rise – Moment-connected	12, 16	Diagonal, Chevron	2, 4	12
PG1-BRB-S	Low-rise – Simply-connected	2, 3, 4	Diagonal, Chevron	2, 4	12
PG2-BRB-S	Mid-rise – Simply-connected	6, 8, 10	Diagonal, Chevron	2, 4	12
PG3-BRB-S	High-rise – Simply-connected	12, 16	Diagonal, Chevron	2, 4	12

[a] Diagonal configurations have a 20 ft bay width, Chevron configurations have a 30 ft bay width. All BRBs are assumed to have bolted brace-to-gusset connections.

[b] Number of braced bays per principal direction

2.4. Estimation of Structural Responses

The structural responses for the archetypes were determined using the SP3 Structural Response Prediction Engine (SRPE) (Cook et al. 2018). The SRPE generates a simplified linear multi-degree-of-freedom model representative of strength and stiffness requirements. Nonlinear response is determined by modal analysis, which is then modified to account for nonlinear behavior of the system. The expected nonlinear behavior is calibrated by sampling from Incremental Dynamic Analysis (IDA: Vamvatsikos and Cornell, 2002) results from high-fidelity nonlinear models with similar linear characteristics.

The SRPE is used to predict peak story drift ratio and peak floor acceleration demands. Residual drifts are computed using the residual drift modeling approach that was developed as part of the ATC-138 project (ATC 2021). Inputs parameters for residual drift modeling are based on two recent analytical studies on BRBFs (Almeter et al. 2018; Vouvakis Manousakis et al. 2024). Details are provided in Section 2.4.5.

The following sections provide an overview of the analytical basis behind the SRPE and the quantification of different Engineering Demand Parameters (EDPs). This section focuses on the prediction of median response conditioned on spectral acceleration (Sa); record-to-record uncertainty and modeling uncertainty are modeled according to FEMA P-58 (FEMA, 2018b).

The structural responses for the archetypes were obtained from the BRBF module of the Structural Response Prediction Engine (SRPE) developed previously for CoreBrace (Almeter et al. 2017, 2018). This sub-section provides an overview of the analytical basis behind the SRPE as well as the quantification of different Engineering Demand Parameters (EDPs). More detailed information can be found in Almeter et al. (2017, 2018).

2.4.1. Analytical Basis Behind the BRBF SRPE

The BRBF SRPE is based on calibration to 90 different variants modeled and analyzed in *OpenSees* (McKenna et al. 2010). The models were based on 15 designs used for FEMA P695 (FEMA, 2009) assessment of BRBF buildings (NIST, 2010) ranging from 1 to 18 stories.

Bracing layouts considered single diagonal and 2-story X configurations. All buildings were designed according to Seismic Design Category (SDC) D_{max} per FEMA P695. Each building design had six variations to investigate the effects of:

- Including a backup frame with moment-connected beam-to-column connections;
- Including the gravity system; and
- Base fixity of BRBF columns.

A summary of the building heights and BRBF bay lengths is provided for each brace configuration in Table 13. A summary of each of the six variations for each building design is provided in Table 14.

Table 13. Building heights and bay widths for building models used in developing the BRBF SRPE (Almeter et al. 2017).

Single Diagonal Bracing	
No. Stories	**Bay Width [ft]**
1	25
2	15
3	25
4	15
6	15
9	15
12	15
18	15

2-Story X Bracing	
No. Stories	**Bay Width [ft]**
2	20
2	30
3	30
6	30
12	20
12	30
16	30

Table 14. Variants for each building used for BRBF SRPE development (Almeter et al. 2017).

Variant	**Backup Frame**	**Base Connection**	**Gravity System**
1	None	Pinned	None
2	None	Pinned	Present
3	Present	Pinned	None
4	Present	Pinned	Present
5	Present	Fixed	None
6	Present	Fixed	Present

Bracing configurations in the archetypes used in the functional recovery study (see section 2.3) are somewhat different than those that were used to develop the SRPE. While these differences in configuration impact component fragilities and local detailing of the frames, they do not impact global responses, e.g. the SRPE does not distinguish between chevron and 2-story X frame response.

Building models were created as two-dimensional representations of single BRBF bays. BRB properties including strain hardening parameters (e.g., ω and β) and stiffness modification factors

(KF) were obtained from design guides provided by CoreBrace. BRBs were modeled as truss elements with a Menegatto-Pinto steel material (*SteelMPF*; Menegatto and Pinto, 1973; Filippou et al. 1983) with isotropic strain hardening. BRB hysteresis was calibrated using the qualification loading protocol defined in AISC 341-16 Section K3.4c (AISC, 2016). Nonlinear models of BRBs do not capture the possibility of weld damage in gusset plates or out-of-plane behavior of gusset plates. Where applicable, nonlinear beam and column hinges were modeled according to Chapter 4 of NIST GCR 17-917-46v2, *Guidelines for Nonlinear Structural Analysis for Design of Buildings Part IIa – Steel Moment Frames* to define the backbone parameters (Lignos and Krawinkler, 2011; Hartloper and Lignos, 2016; NIST, 2017). Nonlinear beam and column hinges were modeled using the *BiLin* material (Ibarra et al. 2005) using monotonic backbones combined with cyclic degradation properties proposed by Lignos and Krawinkler (2011). Simple (non-moment) connections within the BRBF were modeled as pins, where applicable. Gravity system modeling, where applicable, used a lumped "fishbone frame" (Lignos et al. 2013) that includes the nonlinear behavior of gravity connections tributary to the BRBF and acts as a P-Delta "leaning column" to include second order effects of the tributary gravity load. Gravity connections consider the presence of the floor slab and are modeled using the *Pinching4* material (Lowes et al. 2003) with properties calculated according to ATC-114/NIST guidelines (Liu and Asteneh, 2004; NIST, 2017). A graphic representation of a 6-story BRBF model (without backup moment connections) and a gravity system is illustrated in Figure 12.

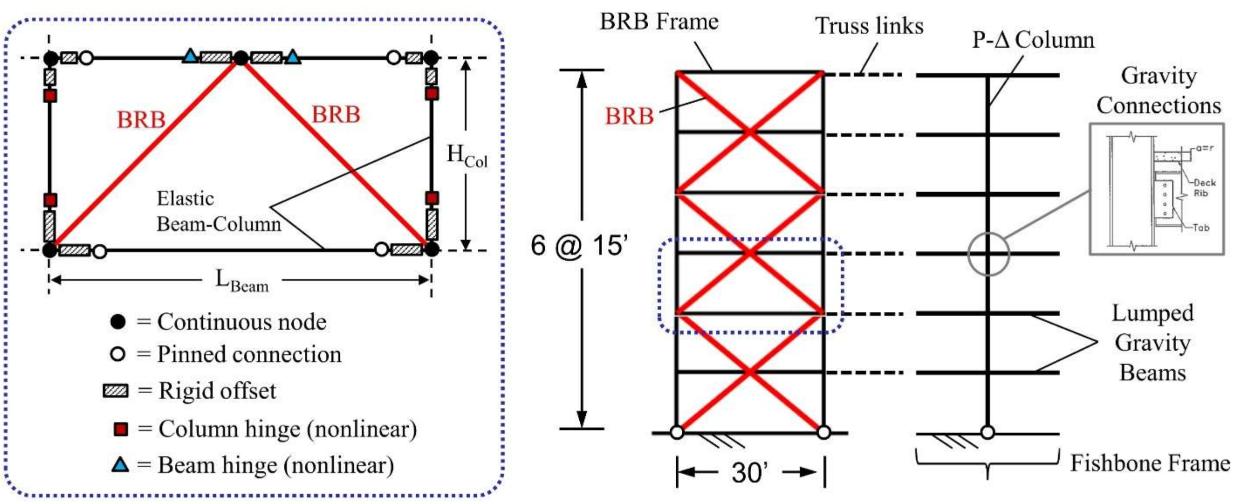

Figure 12 – Illustration on nonlinear modeling used to develop the BRBF SRPE (Image from Saxey et al. 2021)

All models were analyzed using the FEMA P695 far-field ground motion set (FEMA, 2009) consisting of 44 ground motions (i.e., 22 horizontal pairs). Incremental Dynamic Analysis (IDA: Vamvatsikos and Cornell, 2002) was used to obtain a range of linear and nonlinear structural responses for calibration.

The key EDPs for structural response prediction of the BRBF system for Safety Critical Structural Damage (SCSD) are story drift ratio and residual drift ratio. An overview of the estimation of these EDPs are discussed in the following sub-sections.

2.4.2. Structural Properties Estimation

Building structural properties are estimated using a linear building model, with strength and stiffness scaled to meet corresponding design requirements. Typical levels of overstrength and overstiffness (e.g., due to expected material properties, etc.) are added after design requirements are satisfied, to provide the best possible estimate of the true strength and stiffness of the LFRS. The commercial version of SP3 also includes additional strength and stiffness contributions from the gravity system and non-structural components, but these are excluded in this study for compliance with the procedures of section A.8.3.6 of the 2026 National Earthquake Hazards Reduction Program (NEHRP) Provisions.

The process begins by determining the design parameters, including spectral values, response modification factor (R), deflection amplification factor (C_d), and related values (e.g., I_e). Next, a target seismic design drift is selected. For drift-controlled systems, such as most moment frames, this target is typically the design drift limit—for example, 2% for risk category II buildings. For strength-controlled systems, the target drift is a realistic value appropriate for the system type and building height; the expected design drift values are based on a database of hundreds of building designs (from archetype buildings in the SP3 SRPE database). Resilient design iterations use the same process with pairs of R_{fr} and Δ_{afr} for a given analysis. Notably, the deflection amplification factor (C_d) is taken equal to R_{fr} and the building importance factor (I_e) is taken as unity per Section A.8.3.6 of the 2026 NEHRP Provisions.

Following this, the period of a representative design model (limited to the lateral force-resisting system, or LFRS) is determined, considering the target seismic drift and stability requirements (ASCE 7-22 Section 12.8.7). This involves constructing a simple multi-degree-of-freedom (MDOF) model that reflects the system's mass and stiffness characteristics. For instance, moment frames tend to be more shear-dominated, whereas walls and braced frames are more flexure-dominated. This approach is based on a method developed by Miranda (Miranda, 1999; Miranda and Reyes, 2002), which uses a stick model having both flexure and shear deformation characteristics to represent the global stiffness properties of the building. The only differences are that the SP3 version utilizes matrix structural analysis—with mass and stiffness matrices—rather than purely analytical equations, and it also incorporates the ability to model rotational flexibility at the base, which was found to be important for capturing elastic mode shapes at the bottom stories. For BRBF's, the global stiffness properties (e.g. flexure vs shear behavior) were calibrated to reproduce the mode shapes of several archetype BRBF designs ranging in height from low-rise to 20 stories tall.

Starting with very low stiffness, the stiffness matrix is systematically scaled (i.e., increased) until the model achieves the target drift or less, while also satisfying stability requirements. Generally, modal response spectrum analysis (MRSA) is used to generate structural properties for buildings that are modern code-compliant, taller than four stories, and located in high or very high seismic areas. For other cases, the equivalent lateral force (ELF) procedure is used. Wind drift checks can be included in this step but were omitted for this study.

Next, the expected strength and stiffness of the LFRS are determined, accounting for overstrength and overstiffness. These properties vary depending on the LFRS type and building height and are calibrated using results from *OpenSees* models and engineering judgment. An additional optional check can be performed to ensure compatibility between strength and stiffness. If the stiffness is found to be too low in relation to the strength and yield drift, it is increased to a reasonable level. Archetypes for this study are developed with and without including the optional strength/stiffness compatibility check.

The final estimates of the first three periods and mode shapes of the building are determined by performing an eigen analysis with the stiffness matrix (including overstiffness described above) and mass matrix. The final estimate of the ultimate base shear strength is determined from design strength and the expected overstrength.

For the BRBF system, the sizing of the BRBs is conducted directly as part of the design automation process, which is used to select the appropriate fragility functions representing the BRBF assemblies (see Section 2.2.1). Sizing is based on input bay geometry and brace configuration (e.g., chevron or diagonal). The required area of the steel core (A_{sc}) is calculated and then used to select the appropriate fragility with respect to core size (e.g., 5 in^2, 10 in^2, etc.) for the given configuration and bay geometry.

2.4.3. Story Drift Ratio

The SP3 SRPE estimates peak story drift ratio at each story, accounting for the first three mode shapes and periods of the building and its peak strength. First, peak roof drift ratio is estimated using a method that is similar to the ASCE 41 method for target roof displacement, but with factors calibrated directly to the *OpenSees* model results; it depends on the fundamental building period, modal participation factor, spectral acceleration, and correction factors for nonlinear behavior. Second, linear modal analysis is performed using the first three modes, and the results are scaled so that the roof drift from the first step is reproduced. If the spectral acceleration demand is large enough to cause yielding in the structure, then the story drifts are adjusted to account for nonlinear demands. Nonlinear demands are adjusted based on an intensity factor $S = S_a/(V_{max}/W)$, where S_a is the first mode spectral acceleration and (V_{max}/W) represents the normalized peak strength of the building using expected properties. Larger values of S (i.e. more damage) result in more drift concentration in the lower stories. The way in which drifts localize as S increases is calibrated to the nonlinear modeling results and depends on the height of the building (i.e., number of stories). An example calibration for a 6-story BRBF model is shown in Figure 13. The solid lines represent the median peak drift profile from nonlinear time history analysis (NRHA) compared to SRPE response shown in thicker dashed lines. The dotted lines show the elastic response profile before adjusting for nonlinear behavior.

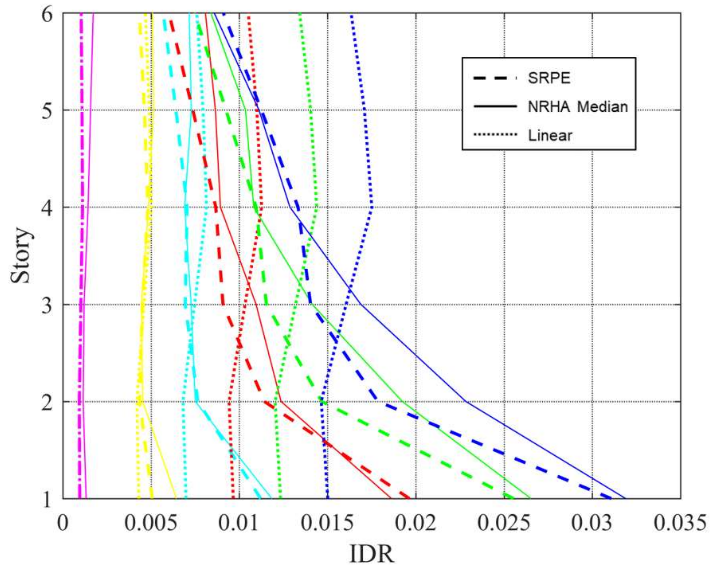

Figure 13. Comparison of SRPE (dashed) and median NRHA (solid) story drift ratio response for a 6-story BRBF. Different colors denote varying levels of intensity. Note, dotted lines represent predicted linear response prior to adjustment for nonlinear behavior.

The BRBF SRPE (Almeter et al. 2017; 2018) for estimating story drift ratios follows a similar procedure to the MRF SRPE developed by Cook et al. (2018), modified for the behavior and physical response of BRBFs. For BRBFs, nonlinear adjustments differ for simply-connected (no backup frame) and moment-connected (with backup frame) beams within the BRBF as well as pinned versus fixed base connectivity conditions. An illustration of an elastic story drift profile compared to an adjusted inelastic profile is shown for an 8-story BRBF in Figure 14. The figure shows that the inelastic profile has distinct regions along the elevation of the building. Region A represents the first story drift up to the location of maximum story drift in elevation. Region B captures the shape of the drift profile in stories above the maximum in elevation. Above Region B, the drift profile can be adjusted to capture any changes in drift demand in uppermost stories, mostly applicable to taller buildings.

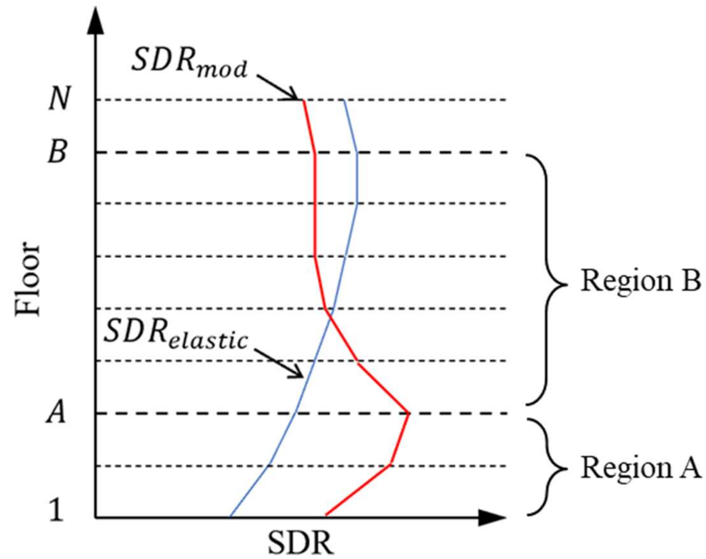

Figure 14 – Elastic and modified inelastic story drift profiles using the BRBF SRPE (Adapted from Almeter et al. 2018)

The building height (e.g., number of stories), presence or absence of a backup frame, and base fixity conditions are used to control the locations of these adjustment regions to best capture the behavior observed from IDA results. BRBFs with less than 6 stories are assumed to exhibit fixed base behavior while those with more than 5 stories are assumed to have pinned base behavior based on the analytical study conducted by Almeter et al. (2017; 2018).

2.4.4. Peak Floor Acceleration

Peak floor acceleration (PFA) is computed based on spectral acceleration, building strength, and the first three modal periods and shapes of the building. First, elastic PFA is computed with modal time-history analysis using FEMA P695 far-field record set scaled to the intensity of interest for every building using the SP3 SRPE. Then, if the spectral acceleration demand is large enough to cause yielding, PFA is adjusted using the intensity factor $S = S_a/(V_{max}/W)$. The amount of reduction of the response depends on how high the story is above the ground, because damage in the lower stories "isolates" the upper stories from acceleration input. An example calibration for a 6-story BRBF model is shown in Figure 15. The solid lines represent the median PFA profile from NRHA compared to SRPE response shown in thicker dashed lines. The dotted lines show the elastic response profile before adjusting for nonlinear behavior. Note that the largest intensity shaking (blue lines) has significant reductions in PFA at upper stories due to damage in the lower stories.

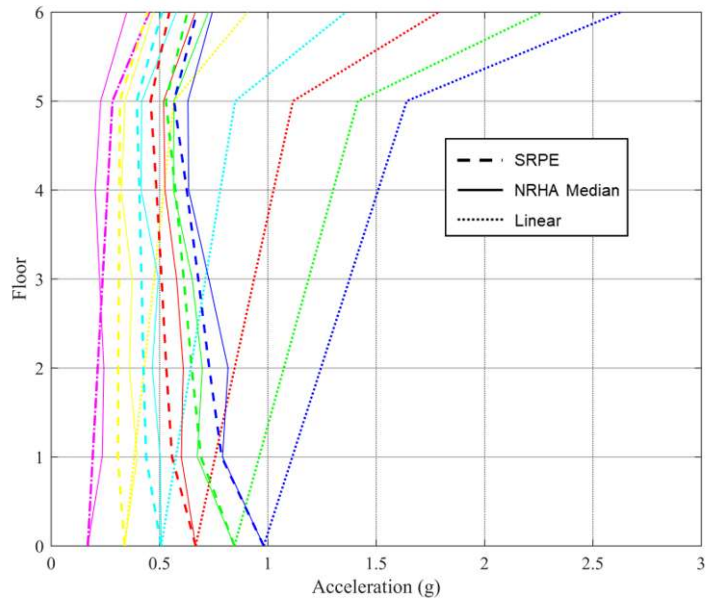

Figure 15. Comparison of SRPE (dashed) and median NRHA (solid) peak floor acceleration response for a 6-story BRBF. Different colors signify varying levels of ground motion intensity. Note, dotted lines represent predicted linear response prior to adjustment for nonlinear behavior.

2.4.5. Residual Drift Ratio

The FEMA P-58 residual drift modeling was updated during the ATC-138 project (ATC, 2021) and resulted in a supplemental FEMA P-58 background document *BD 3.7.26: Updated Model and Criteria for Residual Drift* (DeBock et al. 2024). The revisions to the original FEMA P-58 model allowed for distinctions between structural systems, based on recent analytical studies (Almeter et al. 2018; Vouvakis Manousakis et al. 2024).

The median residual story drift ratio (Δ_r) is estimated from the median transient story drift ratio (Δ) to yield drift ratio (Δ_y). The general format for simplified residual drift estimation has a trilinear form with a transition slope and a primary slope. The initial slope represents the elastic response range (i.e., $\Delta \leq \Delta_y$) where residual displacement is not expected. The transition slope reduces the rate of residual drift accumulation in the region just beyond elastic response to a specified drift ductility, after which, the steeper primary slope accumulates residual drift at a faster rate as peak drift demands increase. The end of the transition region is defined by a system specific drift value Δ_{shift}. An illustration of the basic components of the bilinear residual drift model is shown in Figure 16.

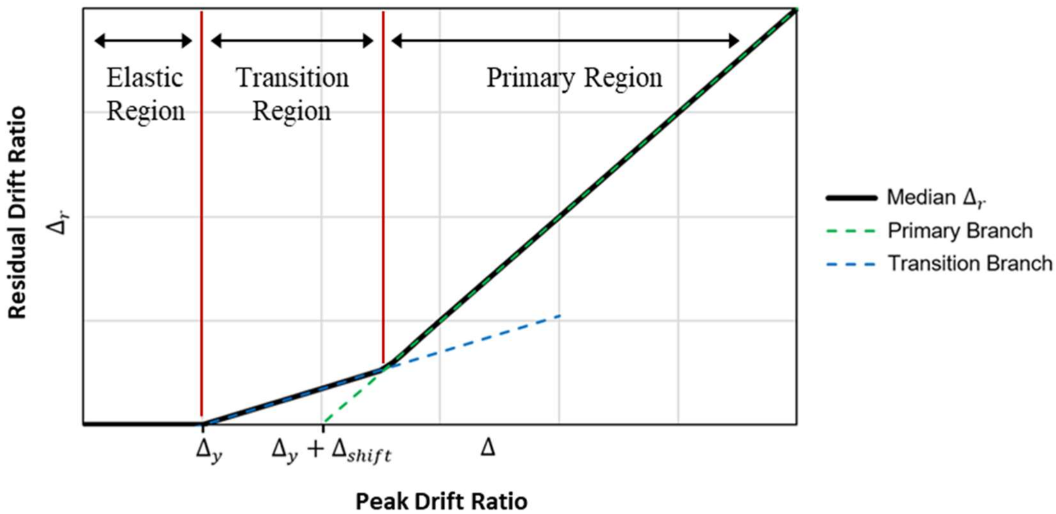

Figure 16 – Basic components of the bilinear model to estimate residual story drift as a function of peak story drift demand and yield story drift.

The revised FEMA P-58 residual drift model provides recommended yield drift ratios (Δ_y) as well as shift values (Δ_{shift}) and slopes for a wide range of structural systems (e.g, MRFs, RC Shear Wall, Braced Frames, and Wood Shear Walls). For BRBF systems, the final model from the ATC-138 project (DeBock et al. 2024) does not distinguish between simply-connected (no backup frame) and moment-connected (with backup frame) systems. This decision was largely based on the findings of Vouvakis Manousakis et al. (2024), which did not show a significant difference in residual drift demands due to the connection type within the BRBF. This finding contrasts with the study conducted by Almeter et al. (2018), which found a significant difference due to beam connectivity in the BRBF. Based on this, the current study adopts the official ATC-138/P-58 model for BRBFs with moment-connected beams, but uses an adjusted version for simply-connected BRBFs. The implemented model for simply-connected BRBFs adjusts the model from Almeter et al. (2018) to account for findings from DeBock et al. 2024, but maintains a distinction between the two types of beam connections in BRBFs.

The residual drift models from Almeter et al. (2018) are compared with those implemented in the current study in Figure 17, with residual drift model parameters provided in Table 15. For moment-connected BRBFs, the revised FEMA P-58/ATC-138 model is used without modification, and is slightly more pessimistic than the Almeter et al. (2018) model, with steeper slopes and a lower transition point (see blue lines in Figure 17). Conversely, the implemented model for simply-connected BRBFs is less pessimistic than the Almeter et al. (2018) model; with a shallower transition slope (see magenta lines in Figure 17).

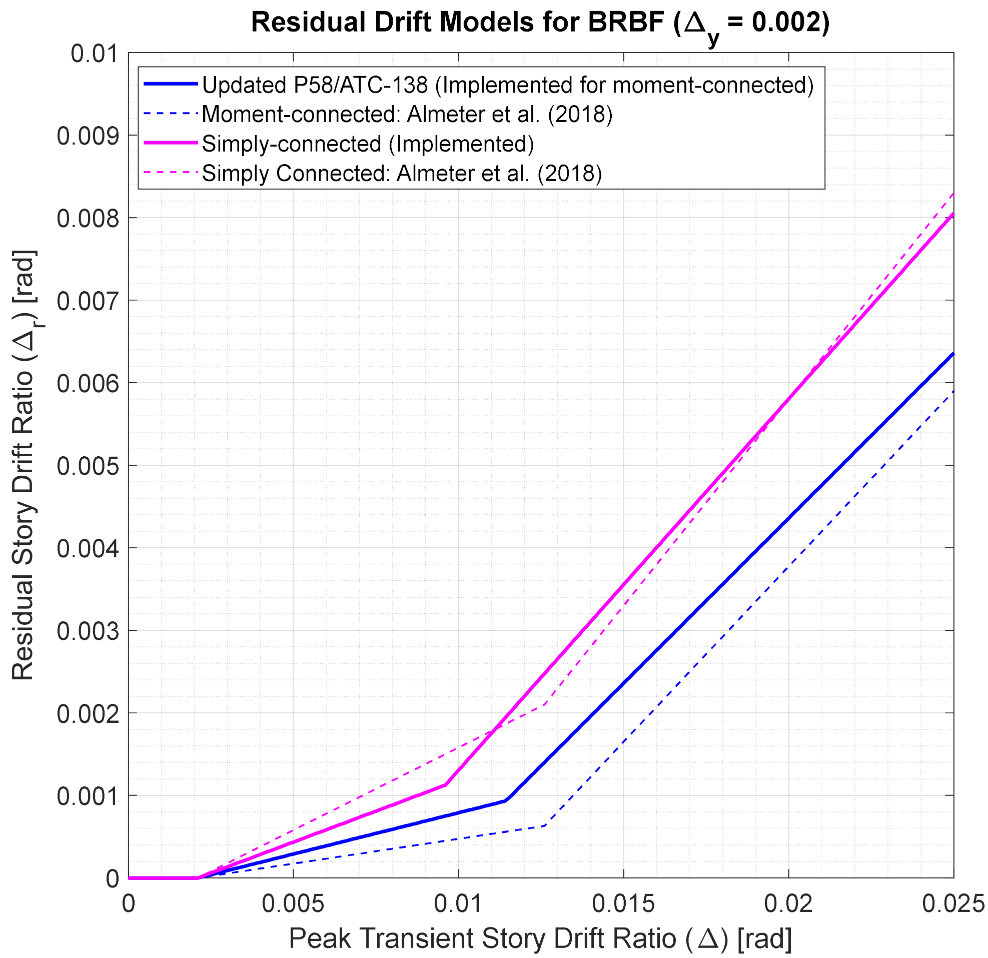

Figure 17 – Comparison of residual drift models implemented in the current study (solid lines) with previous relationships developed by Almeter et al. (2018). Note that ATC-138 updates (solid blue) do not distinguish between simply-connected and moment-connected BRBFs.

Table 15. Residual drift model parameters for BRBF

Connection Type	Source [a]	Δ_{shift} [rad]	Transition Slope	Primary Slope
Moment (with backup frame)	**ATC-138; DeBock et al. (2024)**	**0.007**	**0.10**	**0.40**
	Almeter et al. (2018)	0.013	0.05	0.36
Simple (no backup frame)	**This study (and SP3)**	**0.005**	**0.15**	**0.45**
	Almeter et al. (2018)	0.013	0.17	0.50

[a] **Bold** rows represent models implemented in the current study. Gray rows are previous models used for comparison in Figure 17.

3. RESULTS

The tables and plots below show the R_{fr} and Δ_{afr} envelope for each performance group variant combination. This design envelope identifies the possible design value combinations where all performance groups satisfy both the max and mean analysis criteria. Results are provided separately for both FRC A/B/C acceptance criteria in Section 3.1 and FRC D acceptance criteria in Section 3.2. Additional figures that illustrate general system performance in terms of structural response, controlling component damage and controlling design features are provided in Section 3.3. Full details on the performance of individual archetypes are provided in the attached supplementary materials.

3.1. FRC A/B/C Analysis Results

Table 16 – R_{fr} values across various allowable drift limits required to satisfy the FRC A/B/C structural performance acceptance criteria for each performance group. Analysis results assume increased strength requirements impact building stiffness.

Performance Group	Criteria	Δ_{afr} 0.005	0.0075	0.01	0.0125	0.015	0.0175	0.02
PG1-BRB-M[1]	Max[3]	8	8	6.5	4.5	4.5	4.5	4.5
PG2-BRB-M		8	8	7	4.5	4	4	4
PG3-BRB-M		8	8	8	8	8	8	8
PG1-BRB-S[2]		7.5	6	4	4	3.5	3.5	3.5
PG2-BRB-S		8	6	4.5	3.5	3	3	3
PG3-BRB-S		8	8	8	8	5	5	5
PG1-BRB-M	Mean[3]	8	8	6.5	4	4	4	4
PG2-BRB-M		8	8	7.5	4.5	4	4	4
PG3-BRB-M		8	8	8	8	8	8	8
PG1-BRB-S		7	5.5	4	3.5	3.5	3.5	3.5
PG2-BRB-S		8	6.5	4	3.5	3	3	3
PG3-BRB-S		8	8	8	6	4.5	4	4
Controlling R_{fr} (BRB-M):		8	8	6.5	4	4	4	4
Controlling R_{fr} (BRB-S):		7	5.5	4	3.5	3	3	3

[1]M – Braced frame bay contains fixed welded moment connections
[2]S – Braced frame bay contains pinned beam-to-column connections
[3]In each performance group, the combination of R_{fr} and Δ_{afr} is deemed to be acceptable if the mean P[SCSD] is less than 10%, and the maximum P[SCSD] across all archetypes in the performance group is less than 20%.

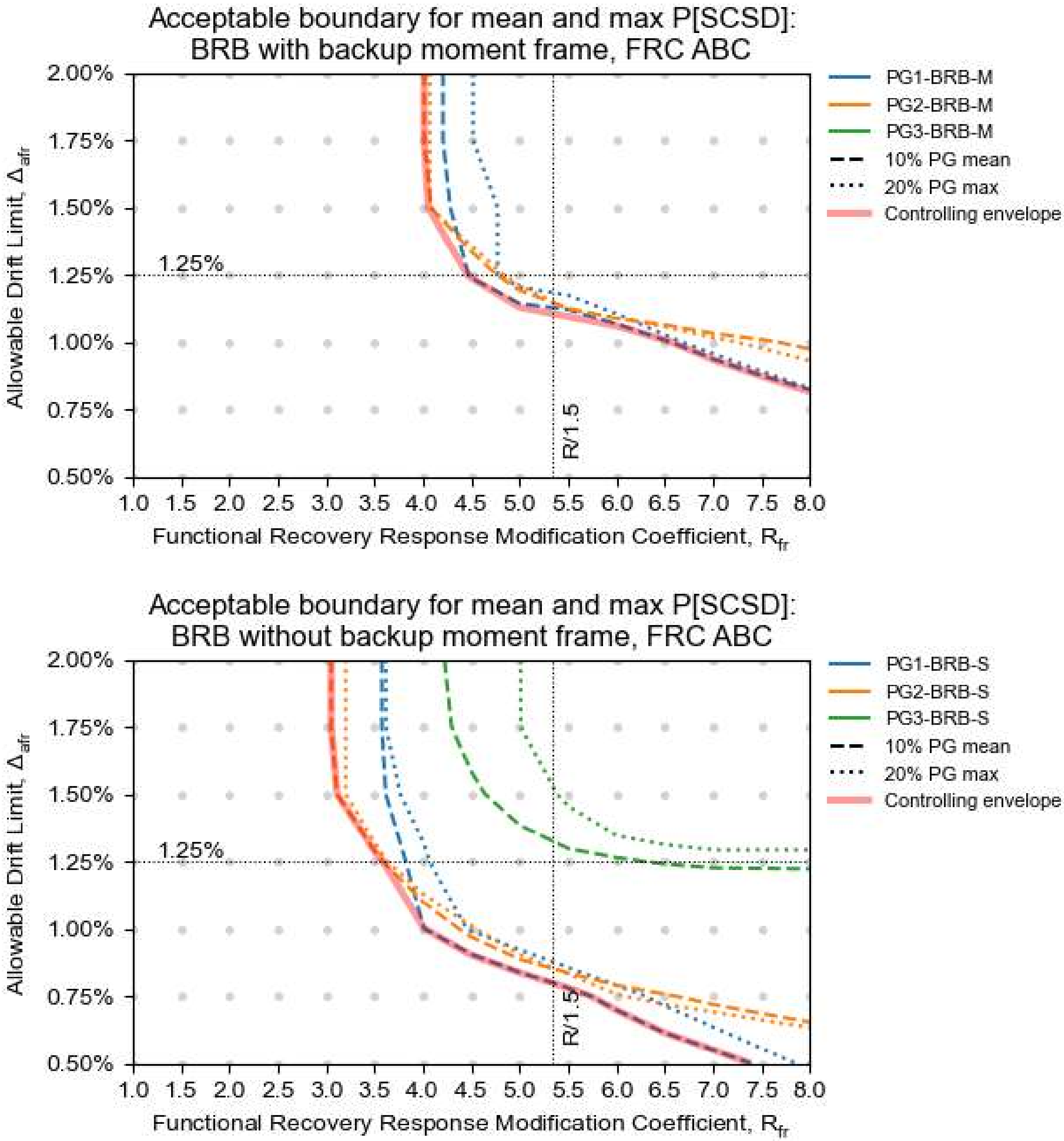

Figure 18 – Combination of R_{fr} and Δ_{afr} values required to satisfy the FRC A/B/C structural performance acceptance criteria for each performance group. Analysis results assume increased strength requirements impact building stiffness.

.

3.2. FRC D Analysis Results

Table 17 – R_{fr} values across various allowable drift limits required to satisfy the FRC D structural performance acceptance criteria for each performance group. Analysis results assume increased strength requirements impact building stiffness.

Performance Group	Criteria	Δ_{afr} 0.005	0.0075	0.01	0.0125	0.015	0.0175	0.02
PG1-BRB-M[1]	Max[3]	8	8	7	5.5	5	5	5
PG2-BRB-M		8	8	8	5	4.5	4.5	4.5
PG3-BRB-M		8	8	8	8	8	8	8
PG1-BRB-S[2]		8	6.5	4.5	4	4	3.5	3.5
PG2-BRB-S		8	7	4.5	3.5	3	3	3
PG3-BRB-S		8	8	8	8	8	5.5	5.5
PG1-BRB-M	Mean[3]	8	8	7.5	5.5	4.5	4.5	4.5
PG2-BRB-M		8	8	8	5.5	4.5	4.5	4.5
PG3-BRB-M		8	8	8	8	8	8	8
PG1-BRB-S		7.5	6	4.5	4	3.5	3.5	3.5
PG2-BRB-S		8	8	5	4	3.5	3	3
PG3-BRB-S		8	8	8	8	8	5	5
Controlling R_{fr} (BRB-M):		8	8	7	5	4.5	4.5	4.5
Controlling R_{fr} (BRB-S):		8	6	4.5	3.5	3	3	3

[1]M – Braced frame bay contains fixed welded moment connections
[2]S – Braced frame bay contains pinned beam-to-column connections
[3]In each performance group, the combination of R_{fr} and Δ_{afr} is deemed to be acceptable if the mean P[SCSD] is less than 15%, and the maximum P[SCSD] across all archetypes in the performance group is less than 25%.

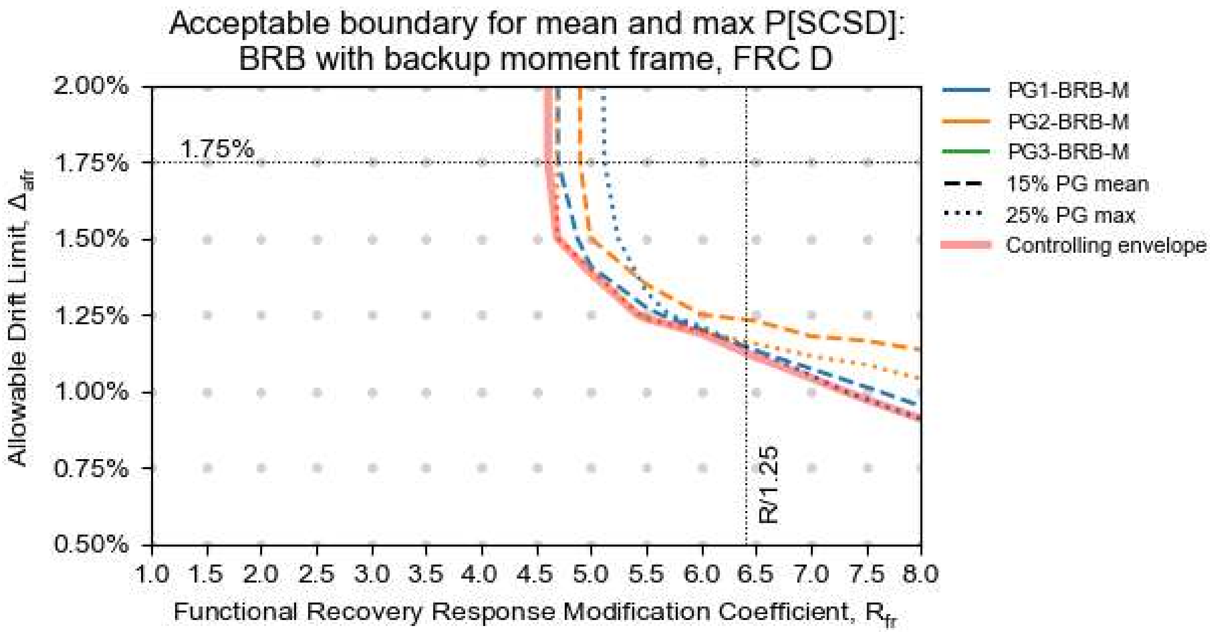

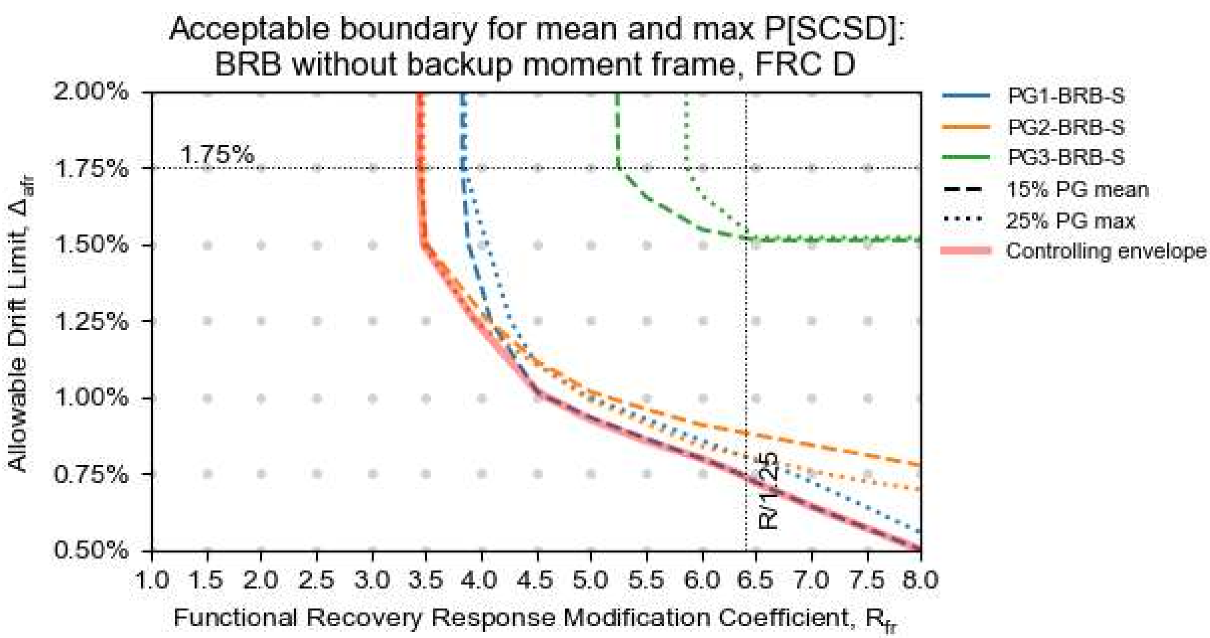

Figure 19 – Combination of R_{fr} and Δ_{afr} values required to satisfy the FRC D structural performance acceptance criteria for each performance group. Analysis results assume increased strength requirements impact building stiffness.

3.3. System Response

The figures below provide detailed insights into the general response and performance outcomes of the models making up each performance group. Figure 20 shows how design drift (Δ_{afr}) relates to median realized drift (x-axis), and how realized drift relates to P[SCSD] (y-axis). The median realized drift is the median peak story drift, in a given story, from all the realizations of peak story drift (~2,000) simulated as part of the FEMA P-58 Monte Carlo assessment. Figure 21 further breaks down the contributions of SCDS by structural component type, and shows that residual drifts are dominant in many of the performance results for BRBF buildings. Finally, Figure 22 shows when the building design transitions from strength-controlled to stiffness-controlled for various R_{fr} and Δ_{afr} combinations. All results presented in this section are general to the response of the system and not specific to Functional Recovery Category.

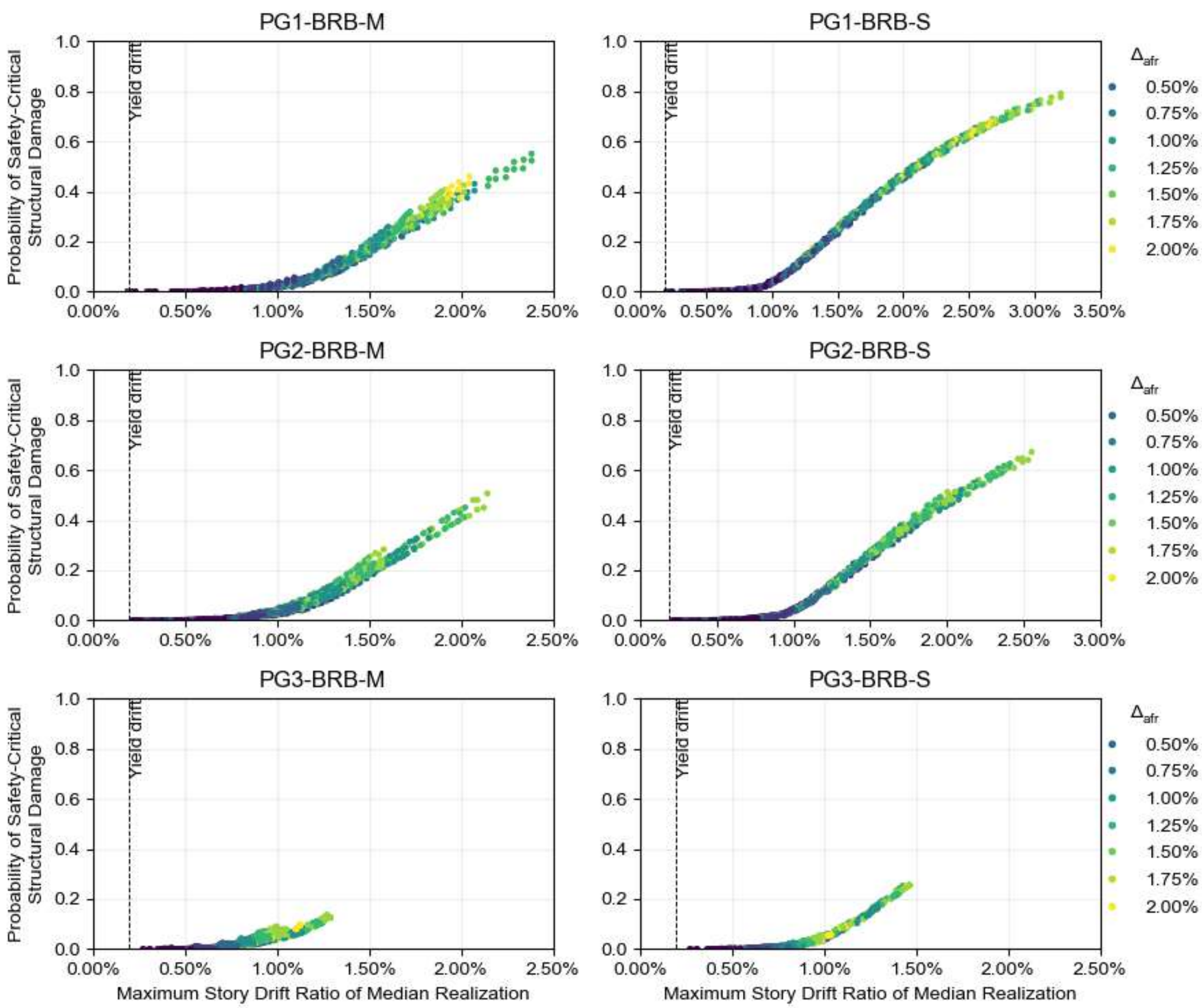

Figure 20 - Relationship between peak realized drift (median) and P[SCSD] for all archetypes.

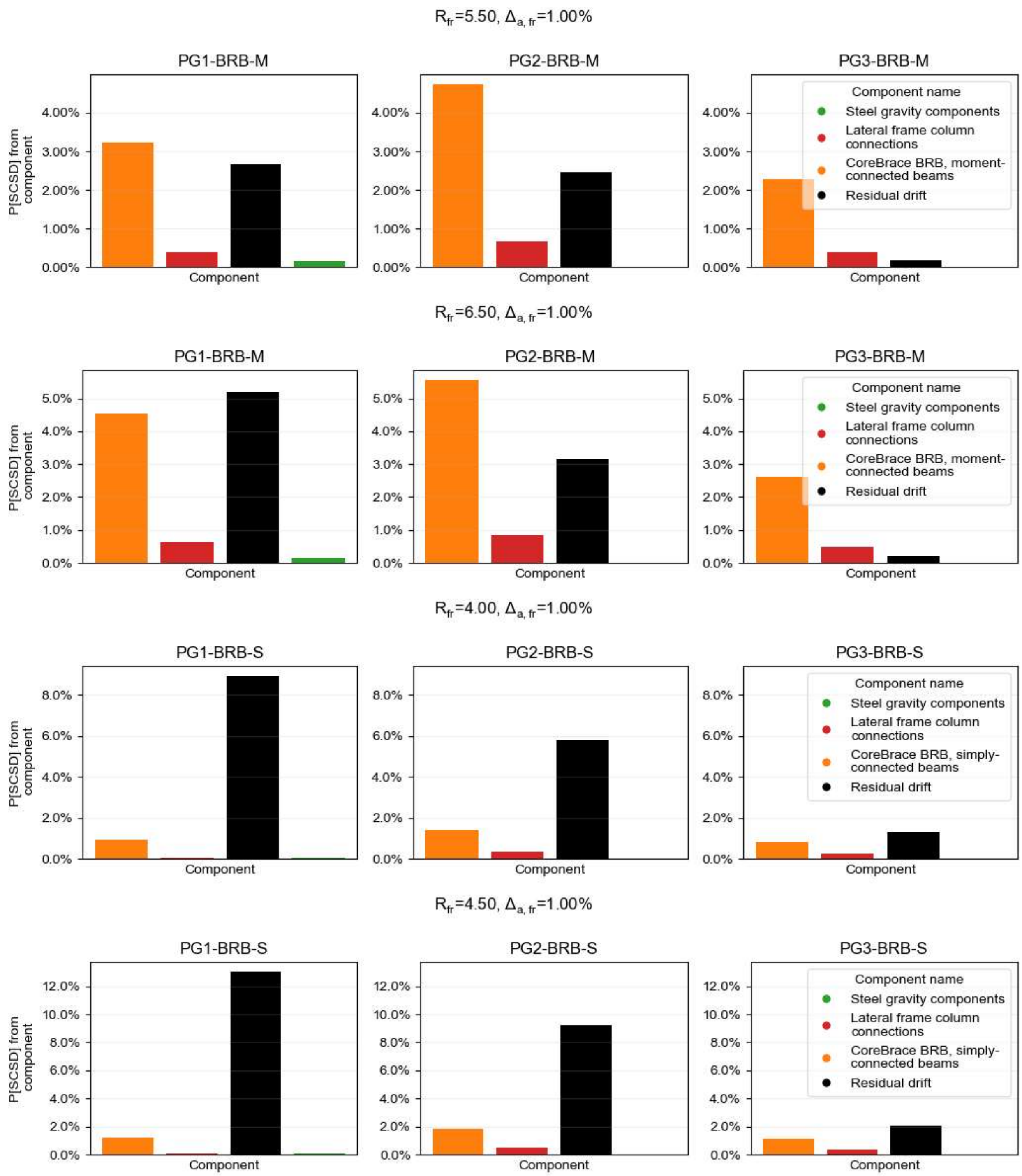

Figure 21 – Component damage contribution to P[SCSD] for each performance group at the recommended design points for each FRC-system combination

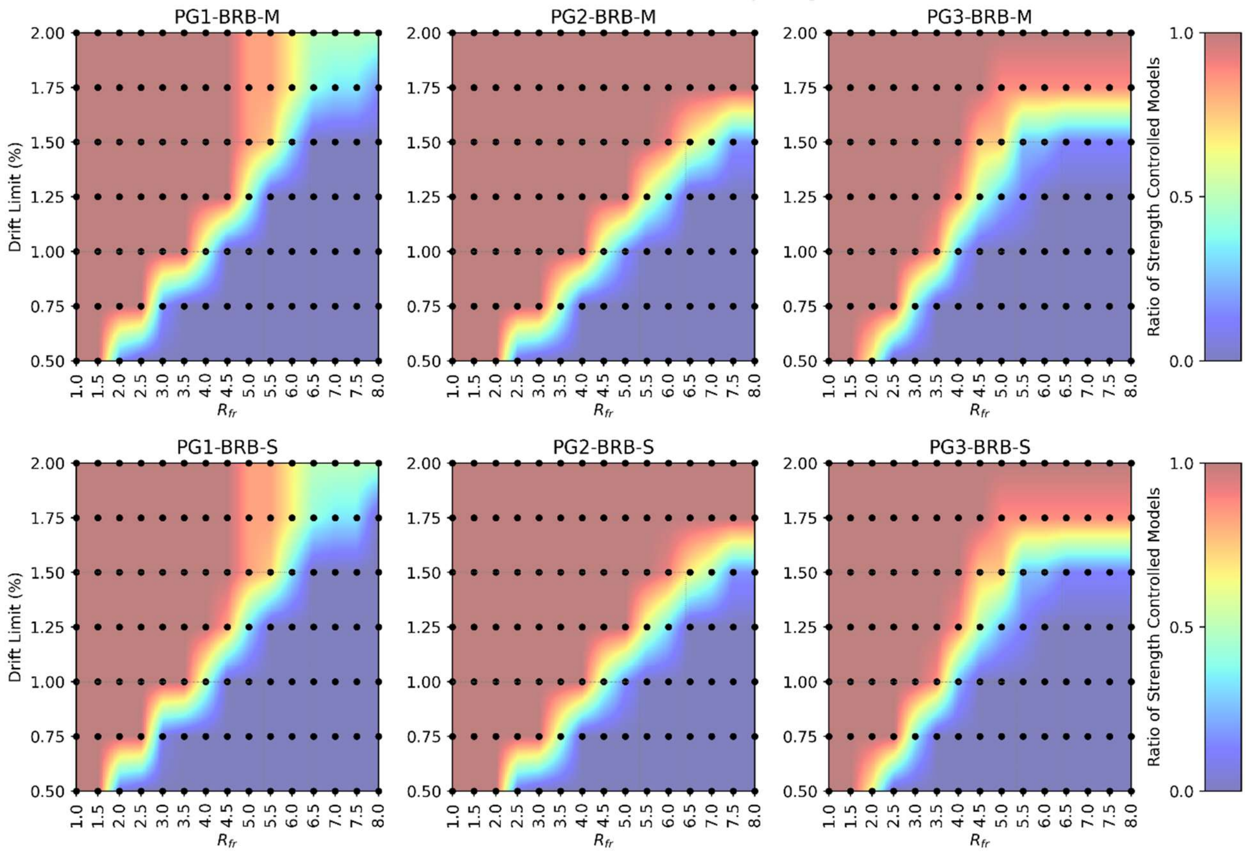

Figure 22 – Average influence of strength on building stiffness for various design requirement combinations assessed. Red coloring indicates that 100% of the models at this design point are controlled by strength requirements (e.g., tightening drift limits by one increment will not change performance). Alternately, blue coloring indicates that 100% of the models at this design point are controlled by stiffness requirements.

3.4. Validation of Peak Floor Acceleration Demand Estimates

The prequalification method documented in the 2026 NEHRP Section A.8.3.6 requires that the peak floor acceleration demands be evaluated for all of the structural system archetype design cases, to ensure that the Section A.10.6 peak floor acceleration adequately reflect the actual peak floor acceleration values observed in the nonlinear response-history analysis results. If the peak floor acceleration demands exceed the acceptable limits of Section A.8.3.6, the recommended $R_{\mu fr}$ value is reduced from the baseline $R_{\mu fr}$ value to adequately adjust the peak floor acceleration demands when using the Section A.10.6 equation. The baseline $R_{\mu fr}$ values are calculated in accordance with Section 13.3.1.2 with the following modifications:

1. R_{fr} and Ω_{0fr} are used in lieu of R and Ω_0
2. The value of Ie is taken as 1.0.
3. The lower limit on $R_{\mu fr}$ of 1.3 in Equation 13.3-6 does not apply.

The recommended Rufr values are determined by checking for compliance with the following two criteria:

1. The ratio of the median peak floor acceleration from analysis averaging across all structural levels to the seismic floor acceleration determined in accordance with Section A.10.7 averaged across all structural levels is computed. The average of this ratio across all archetypes within a performance group shall not exceed 1.0.
2. The ratio of the largest peak floor acceleration from analysis at any level to the largest seismic floor acceleration determined in accordance with Section A.10.7 at any structural level is computed. The average of this ratio across all archetypes within a performance group shall not exceed 1.2.

This Section A.8.3.6 evaluation was completed, resulting in the following $R_{\mu fr}$ requirements:

- For BRBF buildings with pinned-connected frames:
  - $R_{\mu fr}$ = 1.15 is required for FRC A/B/C (based on design using R_{fr} = 5.5 and Δ_{afr} = 0.75%), which is a reduction from the baseline value of $R_{\mu fr}$ = 1.33.
  - $R_{\mu fr}$ = 1.20 is required for FRC D (based on design using R_{fr} = 6.0 and Δ_{afr} = 0.75%), which is a reduction from the baseline value of $R_{\mu fr}$ = 1.41.
- For BRBF buildings with moment-connected frames:
  - $R_{\mu fr}$ = 1.25 is required for FRC A/B/C (based on design using R_{fr} = 5.5 and Δ_{afr} = 1.0%), which is a reduction from the baseline value of $R_{\mu fr}$ = 1.50.
  - $R_{\mu fr}$ = 1.25 is required for FRC D (based on design using R_{fr} = 6.5 and Δ_{afr} = 1.0%), which is a reduction from the baseline value of $R_{\mu fr}$ = 1.50.

4. CONCLUSIONS

This report documents the quantification of the functional recovery seismic performance factors for the Buckling-Restrained Braced Frame (BRBF) system in accordance with the proposed Section A.8.3.6 procedures of the 2026 National Earthquake Hazards Reduction Program (NEHRP) Provisions. The recommended functional recovery seismic performance factors for the BRBF systems with fixed and pinned beam-to-column connections are summarized in Table 18 and Table 19, respectively. These include the functional recovery response modification coefficient, R_{fr}, the functional recovery allowable story drift limit, $\Delta_{afr.}$, and the functional recovery structural ductility reduction factor, $R_{\mu fr}$, for estimation of peak floor accelerations.

Results from the assessment showed that the functional recovery performance factors for BRBFs were primarily governed by the need to limit residual drifts in the buildings. This study finds that residual drifts in BRBF's are most influenced by: (1) The drift limit; stiffening the building by reducing Δ_{afr} reduces residual drifts in BRBF buildings, (2) Strength; increasing the strength of BRBF buildings by reducing R_{fr} decreases yielding and drift concentrations in the lower stories, lowering the likelihood of residual drift, (3) Fixed vs. pinned connections of BRBF beams and columns; BRBFs with surrounding framing that uses fixed beam-to-column connections benefit from stronger restoring forces provided by the frame and exhibit greater resistance to residual drift.

The proposed R_{fr} and Δ_{afr} and $R_{\mu fr}$ for the BRBF lateral force resisting system from the qualification assessment are presented in Table 18 and Table 19 for configurations with and without fixed beam-to-column connections, respectively. In selecting the performance factors, preference was giving to performance factor combinations with tighter drift limits and R_{fr} at or near the judgement-based limit. This approach was taken, because safety-critical structural damage results from excessive displacement and enforcing tighter drift limits is the more direct way to control displacements.

For BRBF's with fixed beam-to-column connections, a drift limit of Δ_{afr} equal to 1% achieves the performance goals for FRC A/B/C and FRC D, without needing to reduce R_{fr} below the judgment-based limits of R/1.5 = 5.5 and R/1.25 = 6.5, respectively; this is listed as Option A in Table 18. Alternatively, a drift limit of Δ_{afr} equal to 1.25% with R_{fr} equal to 4.5 and 5.5 for FRC A/B/C and FRC D, respectively, also satisfies the prequalification acceptance criteria and is listed as Option B in Table 18.

For BRBF's with pinned beam-to-column connections, drift limit of Δ_{afr} equal to 0.75% is required to further limit residual drifts, with R_{fr} equal to 5.5 and 6.0 for FRC A/B/C and FRC D, respectively; this is listed as Option A in Table 19. Alternatively, drift limit of Δ_{afr} equal to 1.0% with R_{fr} equal to 4.0 and 4.5 for FRC A/B/C and FRC D, also meets the performance criteria; this is listed as Option B in Table 19.

The various design options listed in Table 18 and Table 19correspond to the various points along the controlling envelope in Figure 18 and Figure 19 that satisfy the acceptance criteria and are within the judgment-based limits. While both Options A and B satisfy the desired performance criteria, Option A is recommended, because achieving stricter stiffness requirements is expected to be more feasible than meeting stricter strength requirements in BRBF buildings. For FRC D, additional combinations of R_{fr} and Δ_{afr} ranging up to 1.75% are possible; however, these are not recommended because BRBFs are strength controlled in this design range and therefore do not benefit from relaxing the drift limit.

Table 18. Summary of functional recovery seismic performance factors for BRBF-M (with backup frames).

	FRC A/B/C			**FRC D**		
	R_{fr}	**Δ_{afr}**	**$R_{\mu fr}$**	**R_{fr}**	**Δ_{afr}**	**$R_{\mu fr}$**
Analysis results – Design Point Option A	6.5	1.00%	--†	7	1.00%	--†
Analysis results – Design Point Option B	4.5	1.25%	--†	5.5	1.25%	--†
Judgment-based upper limit	5.5	1.25%	n/a	6.5	1.75%	n/a
Recom. Option A – BRBF with fixed framing	**5.5**	**1.00%**	**1.25**	**6.5**	**1.00%**	**1.25**
Option B – BRBF with fixed framing	4.5	1.20%	1.20	5.5	1.25%	1.20

†$R_{\mu fr}$ is only calculated for the recommended seismic performance factors

Table 19. Summary of functional recovery seismic performance factors for BRBF-S (no backup frame).

	FRC A/B/C			**FRC D**		
	R_{fr}	**Δ_{afr}**	**$R_{\mu fr}$**	**R_{fr}**	**Δ_{afr}**	**$R_{\mu fr}$**
Analysis results – Design Point Option A	4	1.00%	--†	4.5	1.00%	--†
Analysis results – Design Point Option B	5.5	0.75%	--†	6.0	0.75%	--†
Judgment-based upper limit	5.5	1.25%	n/a	6.5	1.75%	n/a
Recom. Option A – BRBF pinned framing	**5.5**	**0.75%**	**1.15**	**6.0**	**0.75%**	**1.20**
Option B – BRBF pinned framing	4.0	1.00%	1.15	4.5	1.00%	1.20

†$R_{\mu fr}$ is only calculated for the recommended seismic performance factors

SUPPLEMENTARY MATERIAL

Two supplementary files are attached to this Prequalification Report that provide additional detailed information on the structural response and ATC-138 outcomes from individual archetype models and performance groups, as well as performance outcomes from the independent-strength-and-stiffness check discussed in the body of the report. The general description of the content contained in each file is provided below to assist with navigation and comprehension of detailed results.

- **Analysis Report Tables**
  (*"SupplementalData_AnalysisReportTables_BRBF_final(v1_4b).xls"*)
    - Contains detailed analysis outcomes for each archetype model assessed, including results for FRC A/B/C and FRC D.
    - "Summary" tab provides a summary of the controlling design values and other response metrics for each archetype.
    - "All Runs" tab provides response and performance outcomes for all combinations of model runs for each archetype.
- **Archetype Performance Plots**
  (*"SupplementalData_AnalysisReportTables_BRBF_final(v1_4b).pdf"*)
    - Provides visualizations of analysis outcomes similar to the figures in the report, but for the independent-strength-and-stiffness check.
    - Provides visualizations of analysis outcomes similar to the figures in the report, but for individual archetype models.
    - Provide peak transient drift, residual drift, and peak floor acceleration response profiles for each archetype model.

REFERENCES

AISC. (2016). “Seismic Provisions for Structural Steel Buildings,” *ANSI/AISC 341-16*, American Institute of Steel Construction, Chicago, IL.

AISC. (2022). “Seismic Provisions for Structural Steel Buildings,” *ANSI/AISC 341-22*, American Institute of Steel Construction, Chicago, IL.

Almeter, E. (2017). “Report for Phase I – Structural Response Prediction Method for CoreBrace Buckling Restrained Brace Frame Buildings,” Prepared by Haselton Baker Risk Group for CoreBrace, LLC, West Jordan, UT.

Almeter, E., Wade, K.F., Haselton, C.B., Saxey, B. (2018). “Rapid Risk Assessment of Buckling Restrained Braced Frames, With Focus on Residual Drifts,” *Proceedings of the 11th U.S. National Conference on Earthquake Engineering* (11NCEE), Los Angeles, CA.

ASCE. (2022). “Minimum Design Loads and Associated Criteria for Buildings and Other Structures,” *ASCE/SEI 7-22*, American Society of Civil Engineers, Reston, VA.

ATC. (2021). “Seismic Performance Assessment of Buildings: Volume 8 – Methodology for Assessment of Functional Recovery Time, *ATC-138-3*, Preliminary report for FEMA P-58-8, Prepared by the Applied Technology Council for the Federal Emergency Management Agency, Washington, DC.

Berman, J.W., Bruneau, M. (2009). “Cyclic Testing of a Buckling Restrained Braced Frame with Unconstrained Gusset Connections,” *Journal of Structural Engineering*, 135(12): 1499-1510.

Blowes, K., Molina-Hutt, C., Zimmerman, R., Cook, D.T., Almeter, E., Haselton, C.B. (2025). “Limiting Safety-Critical Structural Damage in Recovery-Based Seismic Design Provisions,” *Earthquake Spectra* (manuscript under review).

Bruneau, M., Mahin, S., Popov, E.P. (1987). “Ultimate Behavior of Butt-Welded Splices in Heavy Rolled Steel Sections,” *EERC Report 87/10*, Univ. of Calif. at Berkeley.

Burda, J.J., Itani, A.M. (1999). “Studies of Seismic Behavior of Steel Base Plates.” *Report No. CCEER 97-7*, Center for Civil Engineering Earthquake Research, Dept. of Civil Engineering, University of Nevada, Reno, Nevada.

Chou, C.-C., Liu, J.-H., Pham, D.-H. (2012). “Steel buckling-restrained braced frames with single and dual corner gusset connections: seismic tests and analyses,” *Earthquake Engineering and Structural Dynamics*, 41: 1137-1156.

Christopolus, A.S. (2005). “Improved Seismic Performance of Buckling Restrained Braced Frames,” *M.S. Thesis*, University of Washington, Seattle, WA.

Cook, D., Wade, K., Haselton, C., Baker, J. W., & DeBock, D. J. (2018). A structural response prediction engine to support advanced seismic risk assessment. In *Eleventh US national conference on earthquake engineering, Los Angeles, CA*.

DeBock, D., Manousakis, I.V., Deierlein, G.G., Zsarnóczay, A. (2024). "Updated Model and Criteria for Residual Drift," *FEMA P-58/BD-3.7.26*, Background documentation for the ATC-138/FEMA P-58 Project, Submitted to the Applied Technology Council, Prepared for the Federal Emergency Management Agency, Washington, DC.

Deierlein, G., Victorsson, V. (2008). "Fragility Curves for Components of Steel SMF Systems," *FEMA P-58/BD-3.8.3*, Background document for the FEMA P-58 project, Submitted to the Applied Technology Council and Prepared for the Federal Emergency Management Agency, Washington, DC.

Fahmy, M. (1999). "Seismic Behavior of Moment-Resisting Steel Column Bases" *PhD Dissertation*, Department of Civil and Environmental Engineering, University of Michigan, Ann Arbor, Michigan.

FEMA. (2009). "Quantification of Building Seismic Performance Factors," *FEMA P695*, Prepared by the Applied Technology Council for the Federal Emergency Management Agency, Washington, DC.

FEMA. (2018). "Seismic Performance Assessment of Buildings: Volume 1 - Methodology," *FEMA P-58-1*, 2nd Edition, Prepared by the Applied Technology Council for the Federal Emergency Management Agency, Washington, DC.

FEMA. (2018b). "Seismic Performance Assessment of Buildings: Volume 2 – Implementation Guide," *FEMA P-58-2*, 2nd Edition, Prepared by the Applied Technology Council for the Federal Emergency Management Agency, Washington, DC.

Filippou F.C., Popov, E.P., Bertero, V.V. (1983). "Effects of Bond Deterioration on Hysteretic Behavior of Reinforced Concrete Joints," *Report EERC 83-19*, Earthquake Engineering Research Center, University of California, Berkeley.

Hajjar, J.F., Lee, D., Dexter, R.J., Grauvilardell, J.E. (2005). "Synthesis of Design, Testing and Analysis on Steel Column Base Plate Connections in High-Seismic Zones," *Structural Engineering Report No. St.-04-02*, Dept. of Civil Engineering, University of Minnesota.

Hartloper, A., Lignos, D.G. (2016). "Updates to the ASCE-41-13 Nonlinear Modeling Provisions for Performance-Based Seismic Assessment of New and Existing Steel Moment Resisting Frames," *M.Eng. Thesis*, McGill University, Montreal, Canada.

Haselton Baker Risk Group (2025). Seismic Performance Prediction Program (SP3).

Ibarra, L.F., Medina, R.A., Krawinkler, H. (2005). "Hysteretic models that incorporate strength and stiffness deterioration," *Earthquake Engineering and Structural Dynamics*, **34**(12): 1489-1511.

Kasai, K., Ooki, Y., Motoyui, S., Takeuchi, T., Kajiwara, K., Sato, E. (2008). "Results of Recent E-Defense Tests on Full-Scale Steel Buildings Part 3 – Experiments on Dampers and Frame Subassemblies," *Proceedings of the 2008 ASCE Structures Congress*.

Lignos, D.G., Krawinkler, H. (2011). "Deterioration Modeling of Steel Components in Support of Collapse Prediction of Steel Moment Frames under Earthquake Loading," *Journal of Structural Engineering*, **137**(11): 1291-1302.

Lignos, D.G., Putman, C., Krawinkler, H. (2013). "Seismic assessment of steel moment frames using simplified nonlinear models," *Computational Methods in Earthquake Engineering*, **30**(0): 91-109.

Lin, P.-C., Tsai, K.-C., Wang, K.J., Yu, Y.-J., Wei, C.-Y., Wu, A.-C., Tsai, C.-Y., Lin, C.-H., Chen, J.-C., Schellenberg, A.H., Mahin, S.A., Roeder, C.W. (2012). "Seismic design and hybrid tests of a full-scale three-story buckling-restrained braced frame using welded end connections and thin profile," *Earthquake Engineering and Structural Dynamics*, 41: 1001-1020.

Lin, P.-C., Tsai, K.-C., Wu, A.C., Chuang, M.-C., Li, C.-H., Wang, K.J. (2015). "Seismic design and experiment of single and coupled corner gusset connections in a full-scale two-story buckling-restrained braced frame," *Earthquake Engineering and Structural Dynamics*, **44**: 2177-2198.

Liu, J., Astaneh-Asl, A. (2000). "Cyclic testing of simple connections including effects of slab," *Journal of Structural Engineering*, **126**(1): 32-39.

Liu, J., Asteneh-Asl, A. (2004). "Moment-rotation parameters for composite shear tab connections," *Journal of Structural Engineering*, **130**(9): 1371-1380.

Lowes, L.N., Mitra, N., Altoonash, A. (2003). "A beam-column joint model for simulating the earthquake response of reinforced concrete frames," *Report No. 2003/10*, Pacific Earthquake Engineering Research Center, University of California, Berkeley.

Menegotto, M., Pinto, P.E. (1973). "Method of analysis of cyclically loaded RC plane frames including changes in geometry and non-elastic behavior of elements under normal force and bending," *Preliminary Report IABSE*, vol. 13.

Miranda, E. (1999). "Approximate seismic lateral deformation demands in multistory buildings," *Journal of Structural Engineering*, **125**(4): 417-425.

Miranda, E., Reyes, C.J. (2002). "Approximate lateral drift demands in multistory buildings with nonuniform stiffness," *Journal of Structural Engineering*, **128**(7): 840-849.

McKenna, F., Scott, M.H., Fenves, G.L. (2010). "Nonlinear Finite-Element Analysis Software Architecture using Object Composition," *Journal of Computing in Civil Engineering*, **24**(1): 95-107.

NIST. (2010). "Evaluation of the FEMA P695 Methodology for Quantification of Building Seismic Performance Factors," *NIST GCR 10-917-08*, National Institute of Standards and Technology, Gaithersburg, MD.

NIST. (2017). "Guidelines for Nonlinear Structural Analysis and Design of Buildings: Part IIa – Steel Moment Frames," *NIST GCR 17-917-46v2*, Prepared by the Applied Technology Council for the National Institute of Standards and Technology (NIST), Gaithersburg, MD.

Nuttayasakul, N. (2001). "Finite element fracture mechanics study of partial penetration welded splices," *Engineer Degree Thesis*, Stanford University.

Palmer, K.D. (2012). "Seismic behavior, performance and design of steel concentrically braced frame systems," *Ph.D. Dissertation*, University of Washington, Seattle, WA.

Saxey, B., Sabelli, R., Welch, D. (2021). "Is Accounting for Gravity Loads in BRBF Design Necessary," *Proceeding of the 2021 SEAOC Convention*, Structural Engineers Association of California, Carlsbad, CA.

Saxey, B. (2024). Personal communication on typical detailing and design of BRBFs, Brandt Saxey, Technical Director, CoreBrace, LLC, July 22, 2024.

Uriz, P., Mahin, S.A. (2008). "Toward Earthquake-Resistant Design of Concentrically Braced Steel-Frame Structures," *Report PEER 2008/08*, Pacific Earthquake Engineering Research Center, University of California, Berkeley.

Vamvatsikos, D., Cornell, C.A. (2002). "Incremental Dynamic Analysis," *Earthquake Engineering and Structural Dynamics*, **31**(3): 491-514.

Vouvakis Manousakis I., Zsarnoczay A., Konstantinidis D., (2024), "Robust Residual Drift Estimation for Seismic Performance Assessment based on High-Fidelity Response Simulation of Steel Frames," (manuscript in preparation).

Wade, K.F. (2017). "FEMA P-58 Fragility Development for CoreBrace Fragility," Prepared by Haselton Baker Risk Group for CoreBrace, LLC, West Jordan, UT.

Welch, D.P., Deierlein, G.G. (2024). "Damage States and Fragilities for Components of Buckling-Restrained Braced Frames," Submitted to CoreBrace, LLC, West Jordan, UT. Findings of the report were directly incorporated into the ATC-138 Project.